**Table 1. Primer sets used for RT-PCR and quantitative real-time RT-PCR**

| Gene | Forward | Reverse |
|---|---|---|
| *Cd3* | 5′-CGAATGTGCCAGAACTGTGT-3′ | 5′-AGTGTCAACAGCCCCAGAAA-3′ |
| Fas ligand (*Fasl*) | 5′-GCCCGTGAATTACCCATGTC-3′ | 5′-TGGAGGAGCCCAAGGAGAA-3′ |
| *Gapdh* | 5′-ATGGGAGTTGCTGTTGAAGTCA-3′ | 5′-CCGAGGGCCCACTAAAGG-3′ |
| Granzyme B (*Gzmb*) | 5′-GGCCCACAACATCAAAGAAC-3′ | 5′-CGCTAGACCTCTTGGCCTTAC-3′ |
| *Ifng* | 5′-GATCCAGCACAAAGCTGTCA-3′ | 5′-GACTCCTTTTCCGCTTCCTT-3′ |
| *Il4* | 5′-TGTACCTCCGTGCTTGAAGA-3′ | 5′-GTGAGTTCAGACCGCTGACA-3′ |
| *Il12* | 5′-AGGTGCGTTCCTCGTAGAGA-3′ | 5′-CCATTTGCTGCATGATGAAT-3′ |
| *Il18* | 5′-ACCGCAGTAATACGGAGCAT-3′ | 5′-GTTGGCTGTTCGGTCGATA-3′ |
| *Nos2* | 5′-TCTGCAGCACTTGGATCAAT-3′ | 5′-AGCTGGAAGCCACTGACACT-3′ |
| MCP-1 (*Ccl2*) | 5′-TGTCTCAGCCAGATGCAGTT-3′ | 5′-TGCTGCTGGTGATTCTCTTG-3′ |
| MDC (*Ccl22*) | 5′-TGGCTCTCGTCCTTCTTGTT-3′ | 5′-TCTTCCACATTGGCACCATA-3′ |
| *Nkrp2* | 5′-TGACATGGCTTGCTGTTTTC-3′ | 5′-TGGTTCCAGGCTTTGTTCTC-3′ |
| Perforin 1 (*Prf1*) | 5′-TTGCGAGGAGAAGAAGAAACA-3′ | 5′-CGGTAGGTCTGGTGGAAAGA-3′ |
| RANTES (*Ccl5*) | 5′-GTGCCCACGTGAAGGAGTAT-3′ | 5′-ACTGCAAGGTTGGAGCACTT-3′ |
| *Tgfb1* | 5′-ATACGCCTGAGTGGCTGTCT-3′ | 5′-TGAAGCGAAAGCCCTGTATT-3′ |
| *Tnfa* | 5′-GTGCCTCAGCCTCTTCTCAT-3′ | 5′-CAATCACCCCGAAGTTCAGT-3′ |

(95°C for 30 s, 60°C for 30 s) after initial denaturation of 95°C for 15 minutes. The primer sequences for PCR are listed in Table 1.

### Transfer of GFP-positive spleen cells into nontransgenic recipients

The EGFP transgenic rats and nontransgenic Wistar rats (all rats were 4 weeks old) were immunized with porcine myosin as described under "Immunization of rats with porcine heart myosin and induction of myocarditis." Mononuclear cells were isolated from the spleen of EGFP transgenic rats one week after immunization and transferred into Wistar rats that had been immunized with myosin 2 weeks before ($1 \times 10^7$/rat intravenously). Five days later, the hearts of the recipients were extirpated, and tissue-infiltrating macrophages were isolated.

### Cytotoxic assay

Six-week-old Wistar rats were immunized with adjuvants containing killed tuberculosis germs. One week later, mononuclear cells were separated from the spleen and incubated in plastic dishes for 20 minutes at 37°C. Resultant adherent cells were collected and then divided into $CD8^-$ and $CD8^+$ cells using the MACS system. These cells were added to the culture of allogenic epithelial thymoma cells (originated from F344 rats carrying the HTLV-I *pX* transgene[19]) with effector-target (E/T) ratios of 30, 10, 1, and 0.1 ($4 \times 10^4$ target cells per well in 24-well plates). After incubation for 18 hours, cytotoxicity was measured using the CytoTox 96 test kit (Promega, Madison, WI).

### Statistical analysis

Data were represented as mean ± standard deviation (SD). Statistical significance between any 2 groups was determined by 2-tailed Student *t* test. *P* values less than .05 were considered to be significant.

## Results

### Expansion of $CD4^+/CD8^+$ cells in the peripheral blood of FW-pX rats with chronic GVHD-like autoimmune diseases

In FW-pX rats, the HTLV-I *pX* transgene induced atrophy of the thymus, resulting in lymphocytopenia, production of autoreactive T cells, and subsequent development of chronic GVHD-like autoimmune diseases.[5] These rats also displayed a compensatory increase in the number of peripheral myeloid cells. To characterize immunophenotypic alterations in their peripheral blood mononuclear cells (PBMCs), we performed 2-color FCM analysis using PBMCs isolated from 6-week-old FW-pX and age-matched control FW-wt rats (Figure 1). The percentages of $CD4^+/CD8^-$ and $CD4^-/CD8^+$ T cells (6.1% and 9.9%, respectively) in FW-pX rats were reduced in comparison with those of FW-wt rats (24.6% and 15.0%, respectively). The reduction of $CD4^+$ T cells was more pronounced than that of $CD8^+$ T cells. On the other hand, $CD4^+/CD8^+$ cells were few in FW-wt rats (3.0%) but markedly increased in number in FW-pX rats (21.0%). In FW-wt rats, $CD4^+$ cells were made up of $CD4^{medium}$ and $CD4^{high}$ populations. By contrast, the majority of $CD4^+/CD8^+$ cells in FW-pX rats expressed CD4 at a medium level. Jefferies et al[6] reported that rat $CD4^{medium}$ and $CD4^{high}$ populations represented monocytes and T cells, respectively, whereas Nascimbeni et al[20] showed that some $CD4^+/CD8^+$ T cells expressed CD4 at a medium level. Thus, we decided to examine whether $CD4^+/CD8^+$ cells in FW-pX rats were monocytes or T cells.

### $CD4^+/CD8^+$ cells in the peripheral blood of FW-pX rats are monocytes

Peripheral blood was obtained from 6-week-old FW-pX rats. At first, we gated $CD4^+/CD8^+$ DP cells and confirmed that these cells

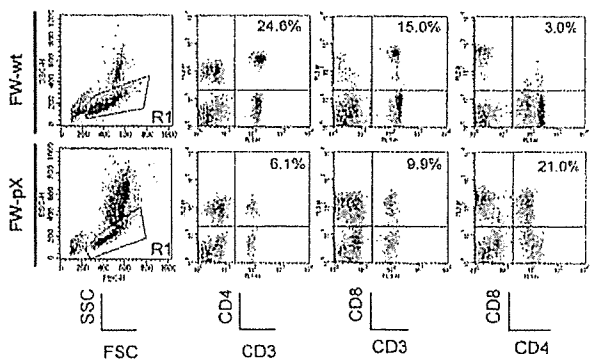


**Figure 1. Expansion of $CD4^+/CD8^+$ cells in the peripheral blood of FW-pX rats.** The top and bottom panels show the results of FCM analyses of peripheral blood from 6-week-old FW-wt (F1 generation of wild-type F344 and Wistar) and FW-pX (F1 generation of HTLV-I *pX* transgenic F344 and wild-type Wistar) rats, respectively. Peripheral blood cells were stained with FITC-conjugated anti-CD3 (G4.18), FITC- or PE-conjugated anti-CD4 (OX-35), and PE-conjugated anti-CD8 (OX-8) Abs, followed by depletion of erythrocytes. At first, the cells were divided based on the forward (FSC) and side scatter (SSC) patterns. Then, PBMCs in region 1 (R1) were gated to analyze the expression of CD3, CD4, and CD8. In both groups, at least 3 rats were examined. Representative data are shown. The numbers in each panel represent the percentage of $CD4^+$ T cells, $CD8^+$ T cells, and $CD4^+/CD8^+$ cells, respectively.

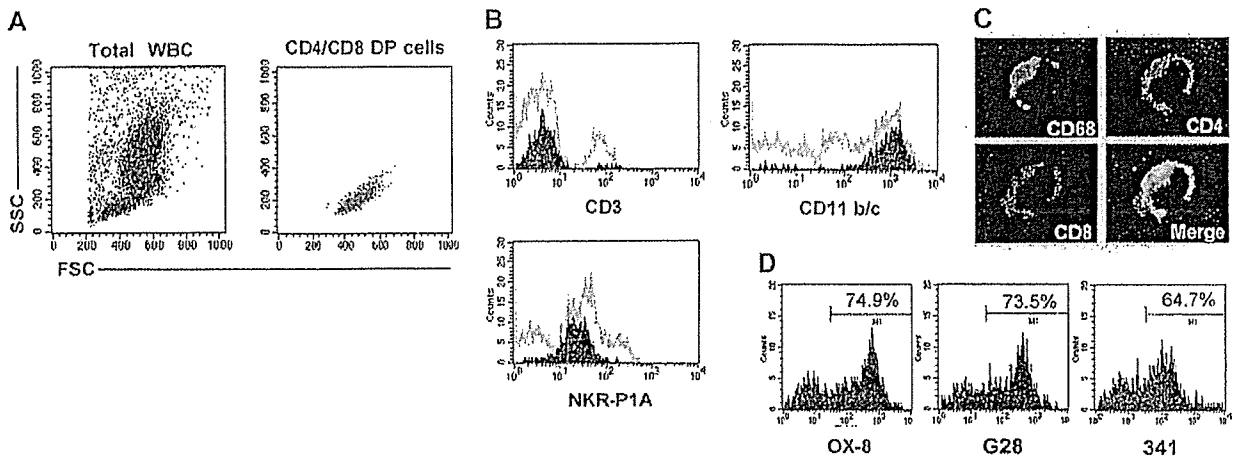


**Figure 2. Characterization of CD4+/CD8+ cells in the peripheral blood of FW-pX rats.** Peripheral blood from 6-week-old FW-pX rats was used. In each experiment, at least 3 rats were used. Representative data are shown. (A) Peripheral blood cells were stained with FITC-conjugated anti-CD4 (OX-35) and PE-conjugated anti-CD8 (OX-8) Abs, followed by depletion of erythrocytes. CD4/CD8 DP cells were gated to confirm that these cells were mononuclear cells. WBCs indicates white blood cells. (B) Peripheral blood cells were stained with FITC- or PE-conjugated anti-CD4 (OX-35), PerCP-conjugated anti-CD8 (OX-8), and FITC- or PE-conjugated anti-CD3 (G4.18), CD11b/c (OX-42), or NKR-P1A Ab (10/78), followed by depletion of erythrocytes. Painted histograms represent the expression of CD3, CD11b/c, and NKR-P1A on CD4+/CD8+ cells. Gray histograms represent the expression of these molecules on total PBMCs. (C) Mononuclear cells separated from the spleen of FW-pX rats were cultured in chamber slides at 37°C for 1 hour. Resultant adherent cells were fixed using cold acetone for 5 minutes and then stained for CD68 (ED-1, green), CD4 (OX-35, red), and CD8 (OX-8, blue). The merged image shows the cell stained with 3 colors (total magnification: × 600). (D) Peripheral blood cells were stained with FITC-conjugated anti-CD4 (OX-35) and PE-conjugated anti-CD8 Abs for the α-chain hinge region (OX-8), α-chain Ig V–like region (G28), or β-chain (341) followed by depletion of erythrocytes. Histograms represent reactivity with the anti-CD8 Abs gated on $CD4^{medium}$ cells.

were mononuclear but not aggregated cells (Figure 2A). Since rat monocytes could not be separated from lymphocytes or NK cells according to the light scatter pattern alone, we examined the expression of surface markers specific for each type of cell. Histograms were obtained by gating of $CD4^+/CD8^+$ cells (Figure 2B). Most $CD4^+/CD8^+$ cells in FW-pX rats were $CD11b/c^{high}$ and $NKR\text{-}P1A^{low}$ but did not express CD3. CD11b/c is expressed on monocytes, granulocytes, and macrophages, thereby known as a marker of myeloid cells.[21] NKR-P1A is highly expressed on NK cells and some T cells but expressed on monocytes at a low level.[22,23] We additionally found that the $CD4^+/CD8^+$ cells did not express OX-62, a marker for DCs[24] (data not shown). These observations suggest that these DP cells have a monocytic but not T, NK, or DC phenotype. To further confirm this suggestion, adherent splenocytes from 6-week-old FW-pX rats were stained for OX-35 (anti-CD4), OX-8 (anti-CD8), and ED-1 (anti-CD68, as a marker for monocytes/macrophages[25,26]) and then observed using a confocal microscope. The 3-color merged image indicates that the DP cells also express CD68 (Figure 2C). It is known that human CD68 can be expressed in activated T and B cells at a low level.[27,28] However, there was no $CD68^+$ population that expressed CD3 or the B-cell marker RLN-9D3 in our rat model. We therefore designated these $CD4^+/CD8^+$ cells as DP monocytes. In addition, we noted that CD4 and CD8 were distributed not only on the cell surface but also in the cytoplasm of DP monocytes. These findings are consistent with the previous observation that CD4 is also expressed in the cytoplasm of human monocytes.[29]

The majority of CD8 molecules are heterodimers composed of α- and β-chains. On the other hand, a subset of T cells and most NK cells are known to express CD8 as homodimers of α-chains.[30] Hirji et al[13] showed that rat alveolar and peritoneal macrophages express CD8 as αβ heterodimers but these CD8 molecules do not react with the anti-CD8 α-chain Ig V–like region Ab (G28). Since the anti-CD8 α-chain hinge region Ab (OX-8) can recognize macrophage CD8, these authors suggested that the Ig V–like region of the CD8 α-chain was masked or modified on rat alveolar and peritoneal macrophages. To analyze the subunit organization of CD8 molecules expressed on the DP monocytes, we performed 2-color FCM analysis using the anti-CD4 (OX-35) and 3 kinds of anti-CD8 Abs, including OX-8, G28, and anti–β-chain Abs (341). Histograms were obtained by gating of $CD4^{medium}$ cells in PBMCs isolated from 6-week-old FW-pX rats (Figure 2D). The percentage of cells reactive with OX-8 (74.9%) was comparable to that stained with G28 (73.5%). The CD8 β-chain was expressed in 64.7% of $CD4^{medium}$ cells. Thus, CD8 molecules expressed on the surface of DP monocytes in FW-pX rats are heterodimers composed of the β-chain and the α-chain with the conserved Ig V–like region.

### Induction of DP monocytes in nontransgenic FW-wt rats

To examine whether DP monocytes are induced exclusively in FW-pX rats carrying the HTLV-I *pX* gene or also in other inflammatory situations unrelated to the transgene, we inoculated porcine myosin into the footpads of 3-week-old FW-wt rats along with the adjuvant containing killed tuberculosis germs. It is known that $CD4^+$ T cells down-regulate their surface CD4 under certain activating conditions.[31] However, we observed no significant down-regulation of CD4 molecules in T cells of our myosin-immunized rats (Figure 3A). The percentages of $CD3^+$ T cells in $CD4^{medium}$ cells were 5.9% and 5.5% in the FW-wt rats with and without immunization, respectively. Thus, we concluded that $CD4^{medium}$ cells were monocytes. One week after immunization, the percentage of $CD8^+$ population in $CD4^{medium}$ cells reached 57.3% ± 6.1% in myosin-immunized FW-wt rats, which was comparable to the proportion observed in 4-week-old FW-pX rats (63.5% ± 6.5%; Figure 3B-C). Four weeks after immunization, the percentage of $CD8^+$ population in $CD4^{medium}$ cells declined to 40.6% ± 7.3% in myosin-immunized FW-wt rats, whereas that in 7-week-old FW-pX rats was maintained at a high level (61.4% ± 4.8%). In 4- and 7-week-old FW-wt rats without immunization, the size of $CD8^+$ population in $CD4^{medium}$ cells was smaller (26.1% ± 14.6% and 23.5% ± 16.3%, respectively). These

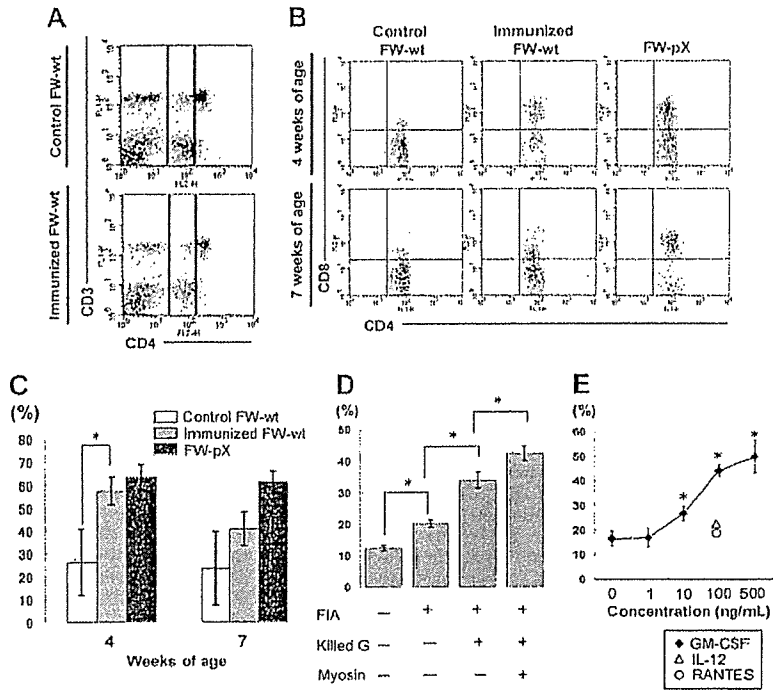


**Figure 3. Induction of CD4/CD8 DP monocytes in nontransgenic rats.** (A) Myocarditis was induced in FW-wt rats by immunization with porcine cardiac myosin and the adjuvant containing killed tuberculosis germs at 3 weeks of age (immunized FW-wt). Peripheral blood was obtained from the FW-wt rats one week after immunization and age-matched controls and then PBMCs in region 1 (R1) were gated as in Figure 1. In both types of rats, the majority of $CD4^{medium}$ cells did not express CD3, thus they were considered to be monocytes. In each group, at least 3 rats were examined. Representative data are shown. (B) The expression of CD8 on peripheral monocytes (practically $CD4^{medium}$ cells) was examined 1 week and 4 weeks after immunization (4 and 7 weeks of age, respectively). Data were compared with those of nonimmunized FW-wt (control FW-wt) and FW-pX rats. In each group, at least 3 rats were examined. Representative data are shown. (C) The percentage of $CD8^+$ cells in monocytes 1 week and 4 weeks after immunization (4 and 7 weeks of age, respectively) is shown as mean ± SD. (D) Inbred F344 rats (3 weeks of age) were immunized with various combinations of components used for the induction of myosin-induced myocarditis. The percentage of $CD8^+$ cells in monocytes was examined 1 week after immunization. In each experiment, at least 3 rats were used. Data are represented as mean ± SD. FIA indicates Freund incomplete adjuvant; Killed G, killed tuberculosis germs. (E) PBMCs from F344 rats (3 weeks old) were incubated with IL-12, RANTES, or GM-CSF under indicated concentrations. We chose these cytokines because they are known to be induced by BCG.[31-33] Twenty-four hours later, the percentage of $CD8^+$ cells in monocytes (practically $CD4^{medium}$ cells) was examined. Data are represented as mean ± SD of repeated experiments done in triplicate. $^*P < .05$.

findings indicate that DP monocytes can be induced in rats without any influence of the *pX* transgene and suggest that they may be induced in an acute inflammatory phase.

To investigate the induction mechanisms of DP monocytes, we next immunized inbred F344 rats with various combinations of individual components used for initial immunization. When rats were immunized with the adjuvant containing killed tuberculosis germs, the percentage of $CD8^+$ population in $CD4^{medium}$ cells was increased in the largest scale, though significant differences were observed by addition of any of the components (incomplete adjuvant only, an increase of 7.7%; adjuvant plus killed tuberculosis germs, an increase of 21.4%; myosin plus adjuvant plus killed tuberculosis germs, an increase of 29.9%; Figure 3D). This suggested that immunization with tuberculosis germs might be critical for the induction of DP monocytes. To test this hypothesis, we examined whether the cytokines and chemokines known to be induced by the recombinant *Mycobacterium bovis bacillus* Calmette-Guerin (BCG)[32-34] can induce DP monocytes in vitro. PBMCs from F344 rats were stimulated with IL-12, RANTES, or GM-CSF for 24 hours and then the percentage of DP monocytes was measured. Among these cytokines/chemokines, only GM-CSF could induce DP monocytes in a dose-dependent manner (Figure 3E). We also observed that the percentage of DP monocytes ($CD4^{medium}$ $CD8^+$ population in PBMCs) was increased from 7.8% to 11.0% by in vivo administration of GM-CSF. However, stimulation of bone marrow cells by GM-CSF failed to induce any significant expansion of $CD4^+/CD8^+$ cells (data not shown).

### Infiltration of $CD4^+/CD8^+$ cells at the site of myocarditis

In myosin-immunized FW-wt rats, myocarditis occurred 3 to 4 weeks after immunization (Figure 4A). At the site of inflammation, macrophages (reactive with ED-1, Figure 4B) infiltrated more abundantly than $CD3^+$ T cells (Figure 4C). To determine if

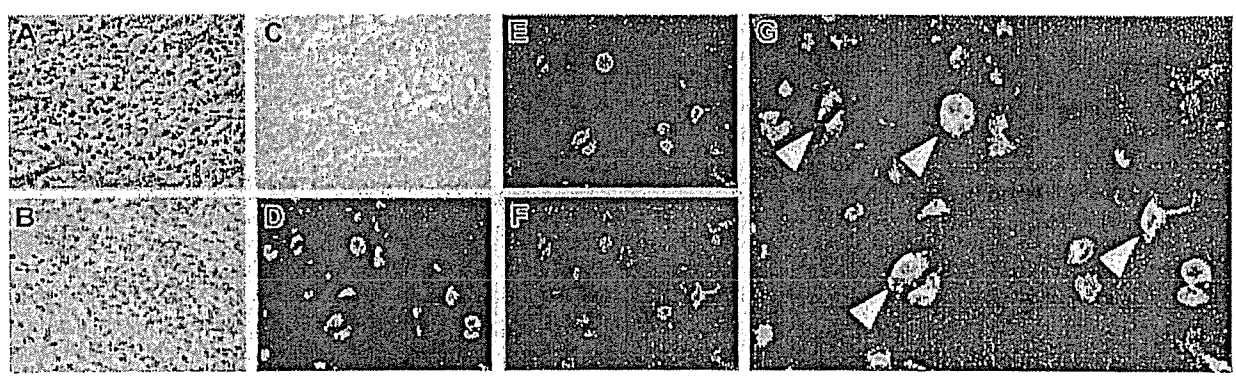


**Figure 4. Infiltration of DP macrophages at the site of myocarditis.** Myocarditis was induced in FW-wt rats by immunization with porcine myosin and the adjuvant containing killed tuberculosis germs at 3 weeks of age. Three weeks later, the heart was extirpated and used for histologic and immunocytochemical examinations. Experiments were repeated twice. Representative results are shown. (A) Hematoxylin and eosin staining. (B-C) Immunohistochemical staining for CD68 (ED-1) and CD3 (IF4), respectively. The cardiac tissues were cut into small pieces and digested with 0.16% collagenase type II. After removal of tissue fragments, cell suspension was incubated in a plastic dish at 37°C. One hour later, adherent cells were harvested and immunofluorescent triple staining was done for CD68 (ED-1, green; D), CD4 (OX-35, red; E), and CD8 (OX-8, blue; F). (G) The merged image. Arrowheads indicate DP macrophages also stained for CD68. Total magnification: × 40 (A-C), × 80 (D-F), and × 200 (G).

infiltrating cells contained DP macrophages, adherent cells were isolated from collagenase-digested cardiac tissues and subjected to immunocytochemical analysis. Half of macrophages (reactive with ED-1) expressed both CD4 and CD8 (Figure 4D-G). These DP macrophages were not reactive with ED-2 (a marker for tissue-resident macrophages[25]) or OX-62 (a marker for DCs; data not shown). Thus, infiltrating DP macrophages are neither tissue-resident macrophages nor DCs but are derived from the blood.

### Cytokine/chemokine profiles and the cytotoxic phenotype of CD4/CD8 DP macrophages

We isolated adherent cells from rat cardiac tissues affected with myocarditis and separated DP macrophages from other, practically $CD8^-$ macrophages (hereafter referred to as $CD8^-$ macrophages) using the MACS system (Figure 5A). We then compared expression profiles of cytokines, chemokines, and cytotoxic factors by quantitative real-time RT-PCR in DP and $CD8^-$ macrophages. DP macrophages showed higher expression of IL-18 (5.2-fold), IFN-γ (2.8-fold), and RANTES (4.8-fold) in comparison with $CD8^-$ macrophages (Figure 5B). By contrast, the expression of MCP-1 was lower in DP macrophages than in $CD8^-$ macrophages (1/4.7-fold). There was no significant difference in the expression of IL-4, IL-12, monocyte-derived chemokine (MDC), or TGF-β, or TNF-α between DP and $CD8^-$ macrophages (data not shown). When we focused on cytotoxic factors, DP macrophages showed significantly higher expression of Fas L (8.0-fold), perforin (9.2-fold), and granzyme B (45.9-fold) compared with $CD8^-$ macrophages (Figure 5C). Expression of iNOS did not show a significant difference between DP and $CD8^-$ macrophages (data not shown). When we examined the expression of Fas L and granzyme B in tissue-infiltrating macrophages by immunohistochemistry, colocalization of these molecules and ED-1 (CD68) was observed (Figure 5D left panels). To rule out the possibility that ED-1–positive ($CD68^+$) cells are overlaid with scattered, secreted granzyme B, we examined the expression of granzyme B in macrophages isolated from the cardiac tissue (Figure 5D right panel). These experiments confirmed that part of ED-1–positive ($CD68^+$) macrophages did express Fas L and granzyme B.

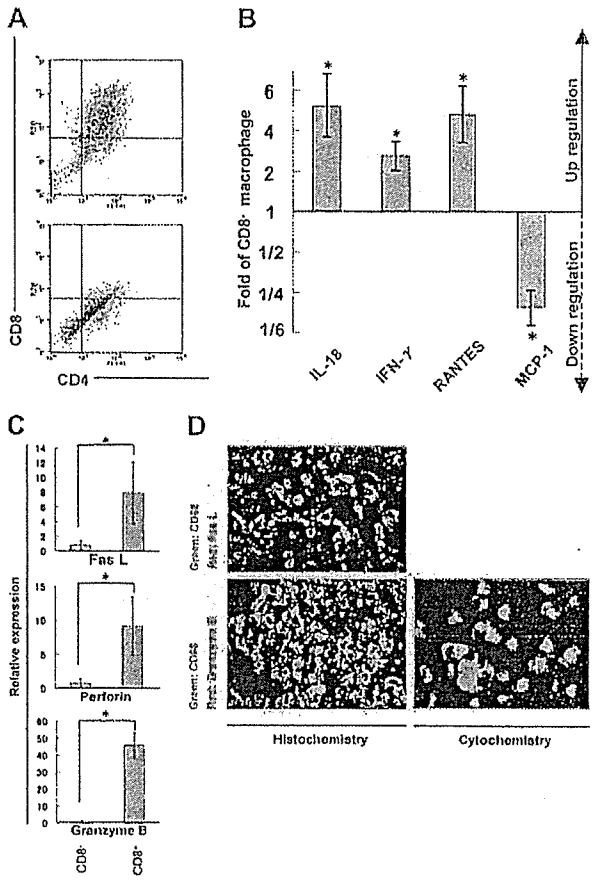


**Figure 5. Expression profiles of cytokines/chemokines and cytotoxic factors in DP macrophages.** Infiltrating macrophages were isolated from the cardiac tissues by collagenase digestion followed by adhesion to the plastic dish. DP macrophages were separated from other macrophages by MACS based on the presence or absence of CD8. Prior to the MACS sorting, we confirmed by light microscopy that macrophages detached from the plastic dish were in a single-cell suspension (data not shown). (A) Macrophages collected from the cardiac tissues were reacted with FITC-conjugated anti-CD4 (OX-35) and PE-conjugated anti-CD8 (OX-8) Abs. MACS was conducted using anti-PE microbeads. The cells selected positively and negatively are shown in the top and bottom panels, respectively. Experiments were repeated at least twice, and representative results are shown. (B) The expression of cytokines/chemokines (IL-18, IFN-γ, RANTES, and MCP-1) in DP macrophages was analyzed by quantitative real-time RT-PCR. The data were compared with those of $CD8^-$ macrophages. Results are represented as a fold (mean ± SD of repeated experiments done in triplicate) against control macrophages. (C) The expression patterns of cytotoxic factors (Fas L, perforin, and granzyme B) in DP macrophages (right columns) were compared with those in $CD8^-$ macrophages (left columns). Data are represented as mean ± SD of repeated experiments done in triplicate. (D) Immunofluorescent double staining for CD68 (ED-1, green) and Fas L (N-20, red), or CD68 (ED-1, green) and granzyme B (N-19, red) in the cardiac tissue section (left panels). Infiltrating macrophages isolated from the tissues were stained for CD68 (ED-1, green) and granzyme B (N-19, red; right panel). Total magnification: × 80. *$P < .05$.

### DP monocytes are precursors of DP macrophages

To determine if DP monocytes in the blood migrated into sites of inflammation and differentiated to DP macrophages, transfer of GFP-positive spleen cells was made into nontransgenic rats immunized with myosin. GFP-positive macrophages were found in cardiac tissues with myocarditis (Figure 6A), and some GFP-positive macrophages expressed both CD4 and CD8 (Figure 6B). Furthermore, when the profiles of DP monocytes and DP macrophages were compared by RT-PCR, the expression patterns of Fas L, perforin, and granzyme B were similar (Figure 6C). On the other hand, the expression of NKR-P2 (rat orthologue of human NKG2D[35]), known to play an important role in killing by NK cells and cytotoxic T lymphocytes (CTLs),[36,37] was higher only in DP macrophages. These findings suggest that DP monocytes are precursors of tissue-infiltrating DP macrophages with a cytotoxic phenotype. In our experiments, evaluation of contaminated $CD8^+$ CTLs was critical. As previously described, the purity of macrophages in the cells recovered from the cardiac tissues with myocarditis was 94% (see "Isolation of macrophages from cardiac tissues, with myocarditis"). We therefore used a mixed cDNA sample (a mixture of $CD8^+$ T cells and fibroblasts in a ratio of 1:9) as a negative control. In this negative control, the expression of CD3, NKR-P2, Fas L, perforin, and granzyme B was hardly detectable, whereas the expression level of the *Gapdh* gene was comparable to that of other samples. Although these experiments do not provide information as to the identity of $CD4^+/CD8^+$ DP cells or assure the absence of contamination of T cells in the samples, they indicate that NKR-P2, Fas L, perforin, and granzyme B are produced by DP monocytes/macrophages. Moreover, immunocytochemistry demonstrated the existence of granzyme B–containing granules in $CD8^+$ $CD68^+$ adherent splenocytes regarded as DP monocytes (Figure 6D).

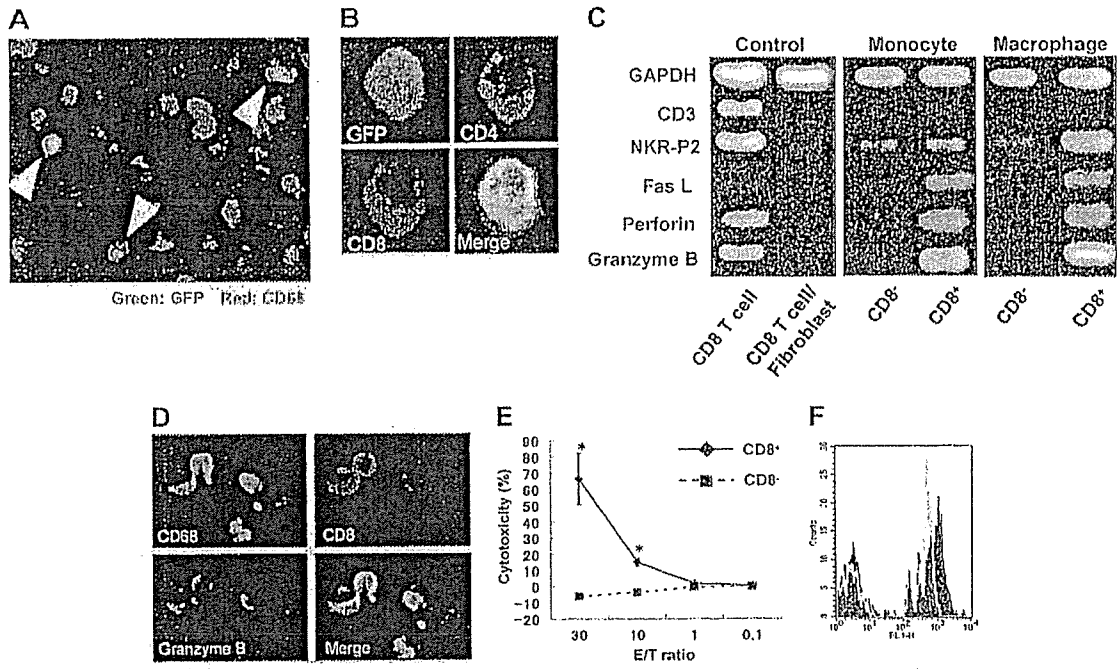


**Figure 6. Origin of CD4/CD8 DP macrophages and function of CD4/CD8 DP monocytes.** (A) GFP-positive spleen cells were transferred into GFP-negative recipients that had been immunized with porcine myosin. EGFP transgenic rats and nontransgenic Wistar rats (all rats were 4 weeks old) were immunized with myosin as described in "Immunization of rats with porcine heart myocin and induction of myocarditis." Mononuclear cells were isolated from the spleen of EGFP transgenic rats 1 week after immunization and transferred into Wistar rats intravenously 2 weeks after immunization ($1 \times 10^7$ cells per animal). Five days later, the hearts of recipients were extirpated, and then tissue-infiltrating macrophages were isolated and used. Experiments were repeated twice, and representative results are shown. Arrowheads indicate cells expressing both GFP and CD68 (ED-1, red). Total magnification: × 100. (B) The cells isolated from the cardiac tissues were cultured in chamber slides at 37°C for 1 hour. Resultant adherent cells were fixed using cold acetone for 5 minutes and then stained for CD4 (OX-35, red) and CD8 (OX-8, blue). The merged image shows that the cell expressing both CD4 and CD8 is also positive for GFP. Total magnification: × 600. (C) FW-wt rats were immunized with myosin and the adjuvant containing killed tuberculosis germs. Mononuclear cells separated from the spleen or cardiac tissues 1 week or 3 weeks after immunization, respectively, were cultured in plastic dishes at 37°C for 1 hour, and then the adherent cells were divided into $CD8^-$ and $CD8^+$ populations, using the MACS system. Expression profiles of CD3, NKR-P2, Fas L, perforin, and granzyme B were compared by RT-PCR. The cDNA from $CD8^+$ T cells served as a positive control. The negative control was the cDNA derived from the 1:9 mixture of $CD8^+$ T cells and fibroblasts. (D) Six-week-old Wistar rats were immunized with adjuvants containing killed tuberculosis germs. One week later, mononuclear cells were separated from the spleen and then cultured in chamber slides at 37°C for 1 hour. Resultant adherent cells were fixed using cold acetone for 5 minutes, followed by staining for CD68 (ED-1, green), granzyme B (red), and CD8 (OX-8, blue). The merged image shows the cells stained with 3 colors. Total magnification: × 200. (E) Cytotoxic assay in vitro. Six-week-old Wistar rats were immunized with adjuvants containing killed tuberculosis germs. One week later, mononuclear cells were separated from the spleen and incubated in plastic dishes for 20 minutes at 37°C. Resultant adherent cells were collected and divided into $CD8^-$ and $CD8^+$ cells using the MACS system. These cells were added to the culture of allogenic epithelial thymoma cells with E/T ratios of 30, 10, 1, and 0.1 ($4 \times 10^4$ target cells per well in 24-well plates). After incubation for 18 hours, cytotoxicity was measured using the CytoTox 96 test kit. Data are represented as mean ± SD of experiments done in triplicate. $^*P < .05$. (F) Phagocytosis assay. Yellow-green carboxylate-modified 1.0 μm latex beads were mixed with peripheral blood from Wistar rats that had been immunized with adjuvants containing killed tuberculosis germs one week before ($1.5 \times 10^7$ beads/300 μL blood). After incubation for 2 hours at 37°C, PE-conjugated anti-CD4 (OX-35) and PerCP-conjugated anti-CD8 (OX-8) Abs were added to the mixture, followed by depletion of erythrocytes. After 3 times wash with cold PBS, $CD4^+/CD8^+$ cells were gated to determine uptake of the fluorescence-labeled beads using FACScan. Experiments were done in triplicate. Representative results are shown. The filled and gray histograms represent the profiles of $CD4^+/CD8^+$ and $CD4^+/CD8^-$ monocytes, respectively.

### Cytotoxic function of DP monocytes

In order to evaluate the function of DP monocytes, we carried out in vitro cytotoxic assays against allogenic tumor cells. As a source of DP monocytes, we used $CD8^+$ adherent splenocytes obtained from Wistar rats that had been immunized with adjuvants containing killed tuberculosis germs. These cells effectively killed epithelial thymoma cells originated from F344 rats carrying the HTLV-I *pX* transgene[19] in a dose-dependent manner (Figure 6E). When the E/T ratio was 30, percent specific lysis was 70.8 ± 6.8. By contrast, $CD8^-$ monocytes hardly killed the tumor cells. These findings clearly indicate that DP monocytes possess a cytotoxic function and that these cells can kill tumor cells without major histocompatibility complex (MHC) restriction.

### Phagocytic ability of DP monocytes

To determine the phagocytic ability of DP monocytes, yellow-green carboxylate-modified 1.0-μm latex beads were mixed with peripheral blood from Wistar rats that had been immunized with adjuvants containing killed tuberculosis germs one week before ($1.5 \times 10^7$ beads/300 μL blood). After incubation for 2 hours at 37°C, uptake of fluorescence-labeled beads in DP monocytes was assayed using FACScan (Figure 6F). The black histogram indicates that the majority of DP monocytes (71.1% ± 4.4%) engulfed the beads during the experimental period. Phagocytic efficiency of DP monocytes was almost equivalent to that of $CD4^+/CD8^-$ monocytes (67.4% ± 8.8%; Figure 6F gray histogram).

### DP monocytes in the human peripheral blood

To examine whether humans also have DP monocytes, we analyzed PBMCs from 12 healthy volunteers by 3-color FCM. $CD4^+/CD8^+$ cells were identified in $CD14^+$ monocytes in all samples examined (Figure 7). The percentage of $CD4^+/CD8^+$ cells in $CD14^+$ monocytes showed considerable individual variations ranging from 17.3% to 1.0%.

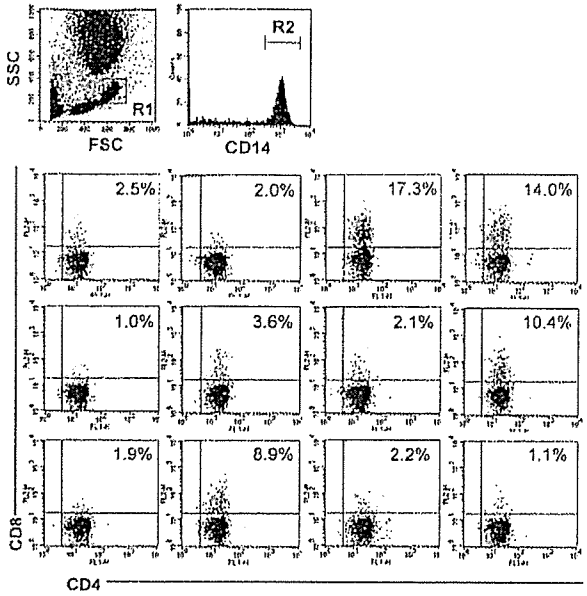


**Figure 7. CD4/CD8 DP monocytes in human peripheral blood.** Human peripheral blood was obtained from 12 healthy volunteers. The cells were stained with FITC-conjugated anti-CD4 (M-T466), PE-conjugated anti-CD8 (HIT8a), and PerCP-conjugated anti-CD14 (MφP9) Abs, followed by depletion of erythrocytes, and then monocytes in region 1 (R1) were gated. The bottom panels show expression of CD4 and CD8 on CD14+ cells in region 2 (R2). The percentage of CD4+/CD8+ cells in CD14+ monocytes is shown in each panel.

## Discussion

In the present study, we have identified a population of monocytes/macrophages characterized by coexpression of CD4 and CD8. This population was originally identified in FW-pX rats carrying the HTLV-I *pX* transgene (Figures 1-2) but later found to be present in wild-type rats (Figure 3). The number of DP monocytes showed a dramatic increase in rats with myosin-induced myocarditis (Figure 3), and the DP macrophages were predominant infiltrating cells at the cardiac lesion (Figure 4). The most notable feature characterizing this population of macrophages is that they express high levels of Fas L, perforin, granzyme B (Figure 5C-D), and NKR-P2 (Figure 6C). In particular, granzyme B was expressed at an extremely high level (45.9-fold) in DP macrophages compared with $CD8^-$ macrophages (Figure 5C). NKG2D is the receptor previously shown to be expressed on NK cells, CTLs, and activated macrophages.[38] It binds to stress-inducible MHC class I molecules, MICA/B, and ULBP/RAET1 in humans and RAE-1 (retinoic acid early inducible-1) in mice.[36,37] NK cells and CTLs bind to the target cells through NKG2D and destroy them through coordinated actions of perforin and cytotoxic factors such as granzyme B. Thus, the collective evidence clearly indicates that tissue-infiltrating DP macrophages exhibit a cytotoxic phenotype. They may therefore contribute to tissue damage by adhering to target cells via their NKR-P2 and secreting perforin and granzyme B.

Another notable feature of CD4/CD8 DP macrophages is that they express IL-18, IFN-γ, and RANTES at higher levels and MCP-1 at a lower level than $CD8^-$ macrophages (Figure 5B). IL-18, IFN-γ, and RANTES induce the T-helper 1 (Th1)–type immune response,[33,39,40] whereas MCP-1 induces the Th2-type immune response.[41] Although we were unable to detect *Cd3* mRNA by RT-PCR in our macrophage samples (Figure 6C), contamination of a small number of T/NK cells cannot be ruled out. Therefore, we should keep in mind the possibility that the cytokine production profiles (Figure 5B) may have been affected by contaminating T/NK cells; this reservation applies especially to IFN-γ, a cytokine typically produced by T/NK cells. However, we can say that tissue-infiltrating DP macrophages are prone to induce IL-18 and Th1-type immune responses at the site of inflammation. Okura et al[42] reported that Th1 cytokines were the major cytokines detected in the early phase of myosin-induced experimental myocarditis in rats. Our present study indicates that DP macrophages infiltrating in the cardiac lesion may enhance the Th1-type immune response observed in the early phase of myosin-induced myocarditis.

The number of DP monocytes showed a dramatic increase by immunization with myosin (Figure 3B-C). When we examined which component in the immunogen was critical for increasing the population of DP monocytes, we found that the killed tuberculosis germs were the most effective factors (Figure 3D). BCG containing killed tuberculosis germs works synergistically with IL-18 for induction of IFN-γ and GM-CSF and induces the Th1-type immune response.[33] GM-CSF increased the number of DP monocytes in a dose-dependent manner in vitro (Figure 3E). These findings suggested that the secretion of GM-CSF induced by immunization with the killed tuberculosis germs triggered the expansion of DP monocytes in peripheral blood. The kinetics of expansion suggest that an increase in the number of DP monocytes occurs in the early phase of inflammation.

To examine whether $CD4^+/CD8^+$ cells are derived from DP monocytes in blood or are generated in situ from resident macrophages, we transferred GFP-positive spleen cells into GFP-negative recipients that had been immunized with myosin in advance (Figure 6A-B). This adoptive transfer experiment clearly indicates that tissue-infiltrating DP macrophages are of hematogenous origin. Consistent with this observation, DP macrophages in situ did not express ED-2 (a marker for tissue-resident macrophages) or OX-62 (a marker for DCs). Thus, overall data indicate that certain stimuli that induce the release of GM-CSF trigger the expansion of DP monocytes in peripheral blood and that these cells migrate to the site of inflammation and differentiate into macrophages displaying the Th1-type immune response and a cytotoxic phenotype. In line with these findings, DP monocytes could kill allogenic tumor cells in vitro (Figure 6E). This killing is unlikely to be mediated by the CTLs contaminated in the effector cells because CTLs can kill only MHC-matched targets. In addition, we demonstrated that DP monocytes were equipped with phagocytic activities comparable to those of $CD4^+/CD8^-$ monocytes (Figure 6F).

Interestingly, human peripheral blood also contains $CD14^+$ monocytes expressing both CD4 and CD8 (Figure 7). In this regard, it is notable that DP macrophage/dendritic cells, which express Fas L more abundantly than other macrophages, have been identified in the thyroid glands of patients with autoimmune thyroid diseases.[43] Although the information available on their surface markers and cytokine profiles precludes us from drawing any conclusions, it is possible that they are derived from the DP monocytes identified in this study.

All volunteers who participated in this study were healthy donors. None of the donors apparently suffered from inflammatory, autoimmune, or neoplastic disorders. It is of great interest to examine whether a population of DP monocytes is increased in

blood under infectious or other disease conditions. Studies along this line are ongoing using clinical samples. Whereas rat DP monocytes displayed cytotoxicity against allogenic tumor cells (Figure 6E), we have thus far been unable to demonstrate cytotoxic activities for human DP monocytes. This may be related to the fact that human DP monocytes were isolated from healthy volunteers, whereas rat DP monocytes were isolated from animals whose immune systems were activated by the transgene or artificial immunization. Studies are in progress to understand whether the rat and human DP monocytes/macrophages have any specialized roles in host defense against infection or cancer and in the pathogenesis of autoimmune disorders.

## Acknowledgments

We thank Ken-ichi Nakase, Chisato Sudo, and Masayo Tateyama for technical assistance.

## References


1. Laskin DL, Weinberger B, Laskin JD. Functional heterogeneity in liver and lung macrophages. J Leukoc Biol. 2001;70:163-170.
2. Stout RD, Suttles J. Functional plasticity of macrophages: reversible adaptation to changing microenvironments. J Leukoc Biol. 2004;76:509-513.
3. Mantovani A, Sozzani S, Locati M, Allavena P, Sica A. Macrophage polarization: tumor-associated macrophages as a paradigm for polarized M2 mononuclear phagocytes. Trends Immunol. 2002;23:549-555.
4. Kikuchi K, Ikeda H, Tsuchikawa T, et al. A novel animal model of thymic tumour: development of epithelial thymoma in transgenic rats carrying human T lymphocyte virus type I pX gene. Int J Exp Pathol. 2002;83:247-255.
5. Baba T, Ishizu A, Ikeda H, et al. Chronic graft-versus-host disease-like autoimmune disorders spontaneously occurred in rats with neonatal thymus atrophy. Eur J Immunol. 2005;35:1731-1740.
6. Jefferies WA, Green JR, Williams AF. Authentic T helper CD4 (W3/25) antigen on rat peritoneal macrophages. J Exp Med. 1985;162:117-127.
7. Wood GS, Warner NL, Warnke RA. Anti-Leu-3/T4 antibodies react with cells of monocyte/macrophage and Langerhans lineage. J Immunol. 1983; 131:212-216.
8. Kim MS, Kim SH, Lee HJ, Kim HM. Expression and function of CD8 alpha/beta chains on rat and human mast cells. Biol Pharm Bull. 2004;27:399-403.
9. Popovich PG, van Rooijen N, Hickey WF, Preidis G, McGaughy V. Hematogenous macrophages express CD8 and distribute to regions of lesion cavitation after spinal cord injury. Exp Neurol. 2003;182:275-287.
10. Shortman K, Liu YJ. Mouse and human dendritic cell subtypes. Nat Rev Immunol. 2002;2:151-161.
11. Hirji NS, Lin TJ, Gilchrist M, et al. Novel CD8 molecule on macrophages and mast cells: expression, function and signaling. Int Arch Allergy Immunol. 1999;118:180-182.
12. Lin TJ, Hirji N, Nohara O, Stenton GR, Gilchrist M, Befus AD. Mast cells express novel CD8 molecules that selectively modulate mediator secretion. J Immunol. 1998;161:6265-6272.
13. Hirji N, Lin TJ, Befus AD. A novel CD8 molecule expressed by alveolar and peritoneal macrophages stimulates nitric oxide production. J Immunol. 1997;158:1833-1840.
14. Torres-Nagel N, Kraus E, Brown MH, et al. Differential thymus dependence of rat CD8 isoform expression. Eur J Immunol. 1992;22:2841-2848.
15. Hirabayash M, Kato M, Aoto T, et al. Offspring derived from intracytoplasmic injection of transgenic rat sperm. Transgenic Res. 2002;11:221-228.
16. Pelidou SH, Zou LP, Deretzi G, et al. Intranasal administration of recombinant mouse interleukin-12 increases inflammation and demyelination in chronic experimental autoimmune neuritis in Lewis rats. Scand J Immunol. 2000;51:29-35.
17. Hayase H, Ishizu A, Ikeda H, et al. Aberrant gene expression by CD25+CD4+ immunoregulatory T cells in autoimmune-prone rats carrying the human T cell leukemia virus type-I gene. Int Immunol. 2005;17:677-684.
18. Bloch G, Toma DP, Robinson GE. Behavioral rhythmicity, age, division of labor and period expression in the honey bee brain. J Biol Rhythms. 2001;16:444-456.
19. Tsuji T, Ikeda H, Tsuchikawa T, et al. Malignant transformation of thymoma in recipient rats by heterotopic thymus transplantation from HTLV-I transgenic rats. Lab Invest. 2005;85:851-861.
20. Nascimbeni M, Shin EC, Chiriboga L, Kleiner DE, Rehermann B. Peripheral CD4(+)CD8(+) T cells are differentiated effector memory cells with antiviral functions. Blood. 2004;104:478-486.
21. Robinson AP, White TM, Mason DW. Macrophage heterogeneity in the rat as delineated by two monoclonal antibodies MRC OX-41 and MRC OX-42, the latter recognizing complement receptor type 3. Immunology. 1986;57:239-247.
22. Scriba A, Schneider M, Grau V, van der Meide PH, Stelniger B. Rat monocytes up-regulate NKR-P1A and down-modulate CD4 and CD43 during activation in vivo: monocyte subpopulations in normal and IFN-gamma-treated rats. J Leukoc Biol. 1997;62:741-752.
23. Kraus E, Lambracht D, Wonigeit K, Hunig T. Negative regulation of rat natural killer cell activity by major histocompatibility complex class I recognition. Eur J Immunol. 1996;26:2582-2586.
24. Brenan M, Puklavec M. The MRC OX-62 antigen: a useful marker in the purification of rat veiled cells with the biochemical properties of an integrin. J Exp Med. 1992;175:1457-1465.
25. Hines JE, Johnson SJ, Burt AD. In vivo responses of macrophages and perisinusoidal cells to cholestatic liver injury. Am J Pathol. 1993;142: 511-518.
26. Dijkstra CD, Dopp EA, Joling P, Kraal G. The heterogeneity of mononuclear phagocytes in lymphoid organs: distinct macrophage subpopulations in the rat recognized by monoclonal antibodies ED1, ED2 and ED3. Immunology. 1985;54:589-599.
27. Hameed A, Hruban RH, Gage W, Pettis G, Fox WM 3rd. Immunohistochemical expression of CD68 antigen in human peripheral blood T cells. Hum Pathol. 1994;25:872-876.
28. Pulford KA, Sipos A, Cordell JL, Stross WP, Mason DY. Distribution of the CD68 macrophage/myeloid associated antigen. Int Immunol. 1990;2: 973-980.
29. Filion LG, Izaguirre CA, Garber GE, Huebsh L, Aye MT. Detection of surface and cytoplasmic CD4 on blood monocytes from normal and HIV-1 infected individuals. J Immunol Methods. 1990; 135:59-69.
30. Moebius U, Kober G, Griscelli AL, Hercend T, Meuer SC. Expression of different CD8 isoforms on distinct human lymphocyte subpopulations. Eur J Immunol. 1991;21:1793-1800.
31. Shin J, Doyle C, Yang Z, Kappes D, Strominger JL. Structural features of the cytoplasmic region of CD4 required for internalization. EMBO J. 1990;9:425-434.
32. Higuchi K, Sekiya Y, Harada N. Characterization of M. Tuberculosis-derived IL-12-inducing material by alveolar macrophages. Vaccine. 2004;22: 724-734.
33. Luo Y, Yamada H, Chen X, et al. Recombinant Mycobacterium bovis bacillus Calmette-Guerin (BCG) expressing mouse IL-18 augments Th1 immunity and macrophage cytotoxicity. Clin Exp Immunol. 2004;137:24-34.
34. Mendez-Samperio P, Vazquez A, Ayala H. Infection of human monocytes with Mycobacterium bovis BCG induces production of CC-chemokines. J Infect. 2003;47:139-147.
35. Alli R, Savithri B, Das S, Varalakshmi C, Rangaraj N, Khar A. Involvement of NKR-P2/NKG2D in DC-mediated killing of tumor targets: indicative of a common, innate, target-recognition paradigm? Eur J Immunol. 2004;34:1119-1126.
36. Verneris MR, Karami M, Baker J, Jayaswal A, Negrin RS. Role of NKG2D signaling in the cytotoxicity of activated and expanded CD8+ T cells. Blood. 2004;103:3065-3072.
37. Diefenbach A, Raulet DH. Strategies for target cell recognition by natural killer cells. Immunol Rev. 2001;181:170-184.
38. Diefenbach A, Jamieson AM, Liu SD, Shastri N, Raulet DH. Ligands for the murine NKG2D receptor: expression by tumor cells and activation of NK cells and macrophages. Nat Immunol. 2000; 1:119-126.
39. Sin J, Kim JJ, Pachuk C, Satishchandran C, Weiner DB. DNA vaccines encoding interleukin-8 and RANTES enhance antigen-specific Th1-type CD4(+) T-cell-mediated protective immunity against herpes simplex virus type 2 in vivo. J Virol. 2000;74:11173-11180.
40. Kawai T, Seki M, Hiromatsu K, et al. Selective diapedesis of Th1 cells induced by endothelial cell RANTES. J Immunol. 1999;163:3269-3278.
41. Gu L, Tseng S, Horner RM, Tam C, Loda M, Rollins BJ. Control of TH2 polarization by the chemokine monocyte chemoattractant protein-1. Nature. 2000;404:407-411.
42. Okura Y, Takeda K, Honda S, et al. Recombinant murine interleukin-12 facilitates induction of cardiac myosin-specific type 1 helper T cells in rats. Circ Res. 1998;82:1035-1042.
43. Nakamura Y, Watanabe M, Matsuzuka F, Maruoka H, Miyauchi A, Iwatani Y. Intrathyroidal CD4+ T lymphocytes express high levels of Fas and CD4+ CD8+ macrophages/dendritic cells express Fas ligand in autoimmune thyroid disease. Thyroid. 2004;14:819-824.

Available online at www.sciencedirect.com
ScienceDirect
Experimental and Molecular Pathology xx (2006) xxx–xxx
Experimental and Molecular Pathology
www.elsevier.com/locate/yexmp

# Enhanced production of p24 Gag protein in HIV-1-infected rat cells fused with uninfected human cells

Jing Chen [a], Xudong Zhao [a], Yurong Lai [a], Akira Suzuki [a], Utano Tomaru [a], Akihiro Ishizu [a,b,*], Akio Takada [a,c], Hitoshi Ikeda [a], Masanori Kasahara [a], Takashi Yoshiki [a,d]

[a] *Department of Pathology, Hokkaido University Graduate School of Medicine, Sapporo 060-8638, Japan*
[b] *Department of Health Sciences, Hokkaido University School of Medicine, Sapporo 060-0812, Japan*
[c] *Sapporo City General Hospital, Sapporo 060-8604, Japan*
[d] *Genetic Lab, Sapporo 060-0009, Japan*

Received 16 August 2006, and in revised form 25 October 2006

**Abstract**

Although many human molecules have been suggested to affect replication of human immunodeficiency virus type 1 (HIV-1), the distribution of such cofactors in human cell types is not well understood. Rat W31/D4R4 fibroblasts expressing human CD4 and CXCR4 receptors were infected with HIV-1. The provirus was integrated in the host genome, but only a limited amount of p24 Gag protein was produced in the cells and culture supernatants. Here we found that p24 production was significantly increased by fusing HIV-1-infected W31/D4R4 cells with uninfected human cell lines of T-cell, B-cell, or macrophage lineages. These findings suggest that human cellular factors supporting HIV-1 replication are distributed widely in cells of lymphocyte and macrophage lineages. We also examined whether the amount of p24 produced by rat–human hybrid cells was correlated with expression levels of specific human genes. The results suggested that HP68 and MHC class II transactivator (CIITA) might up- and down-regulate p24 production, respectively. It was also suggested that HIV-1 replication is affected by molecules other than those examined in this study, namely, cyclin T1, cyclin-dependent kinase 9, CRM1, HP68, and CIITA.


*Keywords:* HIV-1; Rat model; Cell fusion; Cyclin T1; CDK9; CRM1; HP68; CIITA

## Introduction

Replication of human immunodeficiency virus type 1 (HIV-1) is initiated by binding of the viral envelope to the specific surface receptors on target cells. The viral envelope gp120 glycoprotein binds to a human CD4 molecule expressed on T cells and macrophages. A chemokine receptor CXCR4 on T cells or CCR5 on macrophages is also required for virus entry into cells (Kozak et al., 1997). CD4 molecules and chemokine receptors of rodents, which are naturally resistant to HIV-1 infection, do not bind to gp120; therefore, a major barrier to HIV-infection exists at the level of virus entry (Pleskoff et al., 1997). Recent studies showed that rat-derived cells expressing human CD4 and CXCR4 or CD4 and CCR5 became susceptible to HIV-1 viruses (Keppler et al., 2001). However, the rat cell lines produced infectious virus particles still at much lower levels than in human cells, suggesting the existence of additional human factors important for HIV-1 replication.

Over the past couple of decades, several critical steps in HIV-1 replication have been identified. HIV-1 gene expression relies upon complex machinery controlled by two viral regulatory proteins, Tat and Rev. Tat activates the transcription of the viral genome and requires the cellular protein kinase activity termed TAK/P-TEFb, composed of cyclin T1 and cyclin-dependent kinase 9 (CDK9), for its transactivation function (Herrmann and Rice, 1995; Chen et al., 1999). It is reported that the host MHC class II transactivator (CIITA) is recruited instead of Tat during an early phase of

* Corresponding author. Department of Health Sciences, Hokkaido University School of Medicine, Kita-12, Nishi-5, Kita-ku, Sapporo 060-0812, Japan. Fax: +81 11 706 4916.
*E-mail address:* aishizu@med.hokudai.ac.jp (A. Ishizu).

0014-4800/$ - see front matter © 2006 Elsevier Inc. All rights reserved.
doi:10.1016/j.yexmp.2006.11.003

infection (Saifuddin et al., 2000). Rev is necessary for the accumulation of incompletely spliced HIV-1 RNAs in the nucleus and exports them to the cytoplasm cooperating with the cellular exportin 1/CRM1 molecule (Cmarko et al., 2002). During HIV-1 assembly, Gag polypeptides multimerize into immature HIV-1 capsids. The cellular ATP-binding protein, HP68, is required for this process (Zimmerman et al., 2002; Lingappa et al., 2006).

Although many human molecules have been suggested to affect HIV-1 infection and replication, the distribution of such cofactors in human cell types is not well understood. Here we infected rat fibroblasts coexpressing human CD4 and CXCR4 with HIV-1, fused them with uninfected human cell lines of T-cell, B-cell, or macrophage lineages, and then examined virus production and expression profiles of human genes in the fused cells.

## Materials and methods

### *Cells*

Rat W31 fibroblasts (Kanki et al., 2000) were transfected with plasmids carrying the human CD4 gene and those carrying the CXCR4 gene. The expression plasmid of the human CD4 gene (Yamamura et al., 1991) was kindly provided by Dr. Karasuyama (Tokyo Medical and Dental University, Tokyo, Japan). The CXCR4 cDNA was amplified using total RNAs extracted from human peripheral blood mononuclear cells and then subcloned into the pcDNA3.1/Zeo vector (Invitrogen, Carlsbad, CA). Transfection was carried out using Lipofectamine (Invitrogen) according to the manufacturer's protocol. The transfectant, designated as W31/D4R4 cells, was maintained in DMEM supplemented with 10% fetal calf serum (FCS), 400 μg/ml of G418 (GIBCO-BRL, Rockville, MD), and 40 μg/ml of Zeocine (Invitrogen). Several weeks later, cloned W31/D4R4 cells were obtained with limiting dilution.

Human cell lines, including Hut78 and Jurkat (T-cell lymphoma), U937 (macrophage-like cell line), and GI, Raji, Swei, and WT46 (B-cell lymphoma), were cultured in RPMI 1640 medium supplemented with 10% FCS.

### *HIV-1 infection*

W31/D4R4 cells ($5\times10^5$) were pretreated with 2 μg/ml of polybrene for 30 min and then the T-tropic HIV-1 strain, SF33 (Tateno and Levy, 1988), was applied to the cells (equivalent to 200 ng of p24 Gag protein) followed by incubation for 3 h at 37 °C. The supernatants were then removed, and cells were washed 3 times with PBS and digested by trypsin to remove viruses that had not entered the cells. The cells were resuspended in the selection medium and cultured at 37 °C.

### *PCR and RT-PCR for HIV-1 genes*

Genomic DNAs were extracted from the HIV-1-infected W31/D4R4 cells by the standard method. Total RNAs were extracted from the cells with TRIzol Reagent (Invitrogen). The RNAs were subjected to DNase I treatment to remove contaminating DNAs. cDNAs were synthesized with 4 μg of the DNase-treated RNAs using the SuperScript III kit (Invitrogen). PCR for HIV-1 genes was performed using primer sets described previously (York-Higgins et al., 1990; Brandt et al., 1992).

### *ELISA for p24 Gag protein*

HIV-1 p24 Gag protein was quantified using the p24 assay ELISA kit (Zeptometrix, Buffalo, NY). Culture supernatants and cell lysates were subjected to this assay. Tissue culture medium was changed with a fresh one 24 h prior to the assay. The supernatants were centrifuged to remove cell debris; 450 μl of the solution was taken and then mixed with 50 μl of the lysis buffer appended to the kit. The resultant mixture served as culture supernatant samples. For cell lysate samples, $1\times10^7$ cells were resuspended in 450 μl of fresh medium and then mixed well with 50 μl of the lysis buffer. After centrifugation for removal of the pellets, the supernatants were used as cell lysate samples.

### *Cell fusion*

HIV-1-infected W31/D4R4 cells were maintained for 3 months. Cells ($5\times10^6$) were then washed extensively with PBS, digested by trypsin, and mixed with an equal number of human cells. The mixed cell pellets were overlaid with 1 ml of a 50% solution of polyethylene glycol and stirred gently. After incubation at 37 °C for 1 min, PBS was added slowly followed by centrifugation (500×g for 5 min) to remove supernatants. The pellets were resuspended in the selection medium and incubated at 37 °C. The medium was changed with a fresh one every 3 or 4 days. Three weeks later, p24 concentrations were determined in the fused cells and culture supernatants, and the expression of human genes in the rat–human hybrid cells was examined by RT-PCR (see RT-PCR for human genes).

To evaluate the efficiency of cell fusion, human cells were labeled with PKH26 Red Fluorescent Cell Linker Kit (Sigma-Aldrich, St. Louis, MO), according to the manufacturer's protocol, prior to cell fusion. The labeled cells were then fused with uninfected W31/D4R4 cells as described above. Fused cells were incubated in the selection medium at 37 °C for 1 week. The percentage of fused cells was calculated by dividing the number of fluorescence-labeled cells by that of living cells.

### *RT-PCR for human genes*

Expression of human genes, including cyclin T1, CDK9, CRM1, HP68, and CIITA, was examined by RT-PCR. Hybrid cells were harvested 21 days after fusion, and total RNAs were extracted and then subjected to cDNA synthesis. cDNAs were also prepared from parental human cells that were not subjected to fusion with W31/D4R4 cells. The first round of PCR was run for 15 cycles (95 °C for 30 s, annealing for 30 s, 72 °C for 30 s) with sense 1 and antisense 1 primers. The second round of PCR was run for 35 cycles (95 °C for 30 s, annealing for 30 s, 72° for 30 s) with sense 2 and antisense 2 primers. Primer sequences and the annealing temperature are shown in Table 1. These primer sets were specific for the human genes and did not amplify the corresponding rat genes.

Table 1
Primers used for RT-PCR

| Name of genes | | Sequences (5′ to 3′) | Annealing temperature |
|---|---|---|---|
| Cyclin T1 | Sense 1 (2)[a] | agctggaaaatagcccatcc | 60 °C |
| | Antisense 1 | aggaggttctgatggcagag | |
| | Antisense 2 | ctgctggagccacagaattt | |
| CDK9 | Sense 1 | gccaagatcggccaaggcaccttcgg | 56 °C |
| | Sense 2 | ggtgttcaaggccaggcaccgca | |
| | Antisense 1 (2)[a] | cccatcacgagtgataagcacatta | |
| CRM1 | Sense 1 | tgttggagcaagtaggaccag | 55 °C |
| | Sense 2 | gcaatgcatgaagaggacga | |
| | Antisense 1 (2)[a] | cctgaacctgaacgaaatgc | |
| HP68 | Sense 1 | gagttgtcctgtagttcgaatc | 55 °C |
| | Sense 2 | gtacgatgatcctcctgactggc | |
| | Antisense 1 | aactctcctcctgaaagatcttca | |
| | Antisense 2 | tcgttctttaggtgggttaaatca | |
| CIITA | Sense 1 (2)[a] | ctgggattcctacacaatgcg | 60 °C |
| | Antisense 1 | ctgggatcatctcaggctga | |
| | Antisense 2 | tcagcatcgctgttaagaagctc | |

[a] The same primer was used for the first and second rounds of PCR.

Please cite this article as: Chen, J., et al., Enhanced production of p24 Gag protein in HIV-1-infected rat cells fused with uninfected human cells, Exp. Mol. Pathol. (2006), doi:10.1016/j.yexmp.2006.11.003

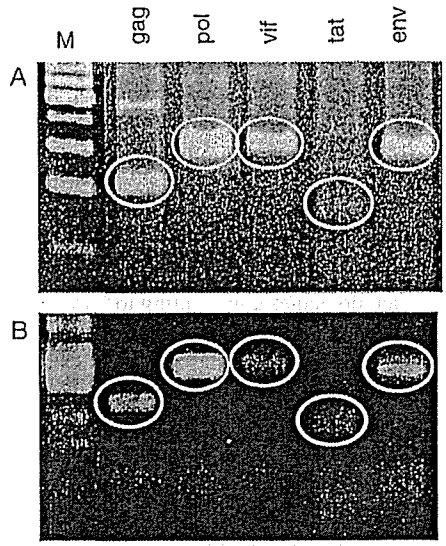


Fig. 1. Integration of the provirus (A) and expression of viral mRNAs (B). W31/D4R4 cells were infected with HIV-1. Genomic DNAs and total RNAs were extracted from the cells 3 months after infection, and then integration of the provirus and expression of viral mRNAs were examined by PCR and RT-PCR, respectively. Ovals indicate specific PCR products. Product size: *gag*, 213 bp; *pol*, 307 bp; *vif*, 321 bp; *tat*, 159 bp; and *env*, 321 bp. M, 100-bp ladder marker.

### *Statistics*

Data were analyzed with Student's *t*-test. *P*-values less than 0.05 were considered to be significant.

## Results

### *Integration and expression of viral genes in W31/D4R4 cells infected with HIV-1*

W31/D4R4 cells were infected with the T-tropic HIV-1 strain, SF33. Three months later, genomic DNAs and total RNAs were extracted from the HIV-1-infected cells, and then integration of provirus and expression of viral mRNAs were examined by PCR and RT-PCR, respectively.

Integration of HIV-1 provirus was confirmed by PCR with 5 pairs of primers, each specific for the *gag*, *pol*, *vif*, *tat*, or *env* region of the HIV-1 genome (Fig. 1A). Expression of viral mRNAs, including *gag*, *pol*, *vif*, *tat*, and *env*, was detected by RT-PCR (Fig. 1B). By contrast, RNAs without reverse transcription did not generate visible PCR products, indicating minimal contamination of genomic DNAs in the RNA sample (data not shown). These findings suggested that W31/D4R4 cells were infected with HIV-1 and that integration of provirus was accomplished and viral mRNAs were expressed in the rat cells.

### *Production of p24 Gag protein in W31/D4R4 cells infected with HIV-1*

We examined the production of viral proteins in HIV-1-infected W31/D4R4 cells by measuring p24 Gag concentrations in the cell lysates and culture supernatants. Samples were collected at days 2, 4, 7, 14, 21, and 28 post-infection, and the amount of HIV-1 Gag protein was measured using the p24 ELISA kit. p24 in the cell lysates showed a peak concentration of >10,000 pg/ml at day 4 post-infection and decreased to 84 pg/ml at day 28 post-infection (Fig. 2). Even 3 months later, p24 in the cell lysates retained a concentration of 12 pg/ml (data not shown). On the other hand, p24 in the supernatants showed a peak concentration of >1000 pg/ml at day 4 post-infection, but decreased rapidly, and fell below the detection limit at day 28 post-infection.

### *Production of p24 Gag protein in fused cells*

Three months after HIV-1 infection, the infected W31/D4R4 cells were fused with human cell lines. Cell lysates and culture supernatants were subjected to ELISA at day 21 after cell fusion. p24 concentration in the cell lysates showed a 4- to 10-fold increase when the HIV-1-infected W31/D4R4 cells were fused with an uninfected human T-cell lymphoma line Hut 78, a macrophage-like cell line U937, and B-cell lymphoma lines GI, Swei, and WT 46 (Fig. 3A). Although there was no statistically significant difference, fusion with the B-cell lymphoma line Raji also increased the concentration of p24 in the cell lysates. On the other hand, no significant increase was seen when HIV-1-infected W31/D4R4 cells were fused with the human T-cell lymphoma line Jurkat.

Fusion with human cells generally failed to increase p24 concentration in the culture supernatants (Fig. 3B). However, p24 concentration showed a slight but statistically significant increase (10 pg/ml) when the HIV-1-infected W31/D4R4 cells were fused with the B-cell lymphoma line WT46.

### *Alteration of human gene expression after cell fusion*

Expression of human cyclin T1, CDK9, CRM1, HP68, and CIITA genes was examined by RT-PCR in both parental

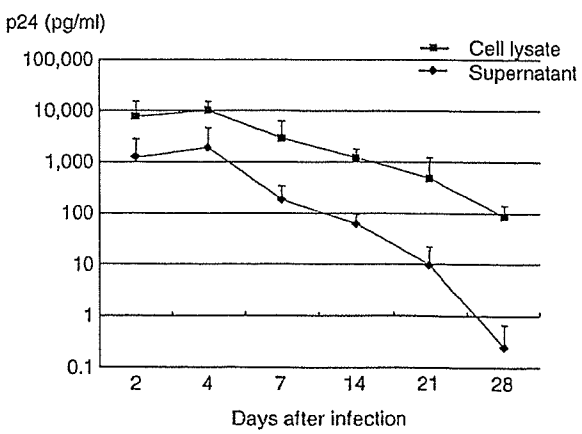


Fig. 2. Production of p24 in HIV-1-infected W31/D4R4 cells. W31/D4R4 cells were infected with HIV-1. Cell lysates and culture supernatants were collected at days 2, 4, 7, 14, 21, and 28 post-infection, and the amount of HIV-1 p24 Gag protein was measured using the ELISA kit.

Please cite this article as: Chen, J., et al., Enhanced production of p24 Gag protein in HIV-1-infected rat cells fused with uninfected human cells, Exp. Mol. Pathol. (2006), doi:10.1016/j.yexmp.2006.11.003

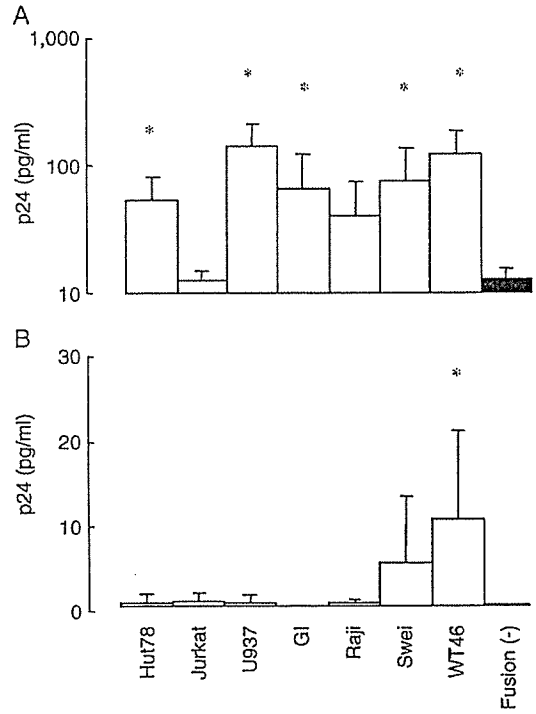


Fig. 3. Production of p24 in HIV-1-infected W31/D4R4 cells fused with uninfected human cells. HIV-1-infected W31/D4R4 cells were fused with indicated human cells. Cell lysates (A) and culture supernatants (B) were subjected to ELISA at day 21 after fusion (*$p<0.05$).

human cell lines and rat–human hybrid cells. For this analysis, we used the same batch of hybrid cells as used in Fig. 3. Cyclin T1, CDK9, CRM1, and HP68 genes were expressed in all the human cell lines examined (Fig. 4, left panels). Notably, expression of CIITA was not detected in Jurkat (see asterisk).

After cell fusion, expression of human genes was largely extinguished (Fig. 4, right panels). None of the hybrid cells expressed human CDK9 or CRM1. Expression of cyclin T1 was seen exclusively in W31/D4R4 cells fused with Raji, and HP68 was expressed only in W31/D4R4 cells fused with WT46. The human CIITA gene, expressed in Hut78, U937, and the B-cell lymphoma lines, lost its expression after fusion. On the contrary, expression of CIITA was induced in W31/D4R4–Jurkat hybrid cells.

## Discussion

Development of a small animal model of HIV-1 infection would greatly facilitate studies of virus transmission, pathogenesis, host immune responses, and antiviral strategies. Mice and rats are attractive models for HIV-1 study because they can be genetically manipulated. However, the development of a permissive model has been hampered by the inability of HIV-1 to infect primary rodent cells.

Rodent CD4 and CXCR4/CCR5 (receptors for HIV-1) do not bind to the viral envelope gp120 (Pleskoff et al., 1997). Transgenic mouse and rat cells, expressing human CD4 and CXCR4 or CD4 and CCR5, became susceptible to HIV-1 infection, and the provirus could be integrated in the host genome (Sawada et al., 1998; Keppler et al., 2001). However, replication of the infectious virus remained at much lower levels in these rodent cells than in human cells, thus suggesting the involvement of additional human genes in virus replication (Freed, 2004; Trkola, 2004). Indeed, it has been reported that human but not rodent cyclin T1 supports the function of viral Tat protein (Keppler et al., 2001). One of the effective ways to identify human molecules contributing to HIV-1 replication is to conduct cell fusion experiments using human and rodent cells. Identification of such molecules and subsequent introduction into rodents should help us establish animal models of HIV-1 infection.

Although several human molecules have been suggested to affect HIV-1 replication, the distribution of such cofactors in human cell types is not well understood. In the present study, rat fibroblasts transgenic for human CD4 and CXCR4 genes, W31/D4R4, were infected with HIV-1. These cells were fused with uninfected human cell lines of T-cell, B-cell, or macrophage origin followed by the assessment of associations between viral production and human gene expression.

As expected, rat W31/D4R4 cells could be infected with HIV-1, and the provirus was integrated in the host genome (Fig. 1A). Expression of virus genes was detectable by RT-PCR even 3 months after infection (Fig. 1B), but the concentration of p24 Gag protein was very low in the cell lysates (12 pg/ml) and was below the detection limit in the culture supernatants (Fig. 2). Poor production of p24 may have occurred because rat cells infected with HIV-1 died or were unable to proliferate like their uninfected counterparts and/or because host factors supporting viral replication were deficient in rat cells. Since we observed no significant difference in the viability and proliferation of W31/D4R4 cells before and after HIV-1 infection, the first possibility appeared unlikely. Thus, we conducted cell fusion experiments using HIV-1-infected W31/D4R4 cells and uninfected human cell lines.

We found significant recovery of the expression of p24 Gag protein in the HIV-1-infected W31/D4R4 cells upon fusion with the human T-cell lymphoma line Hut78, macrophage-like cell line U937, and B-cell lymphoma lines GI, Swei, and WT46 (Fig. 3A). These findings indicate that human factors that support HIV-1 replication are distributed widely in cells of lymphocyte and macrophage lineages.

To examine whether the amount of p24 produced by hybrid cells is correlated with expression levels of specific human genes, we analyzed expression of cyclin T1, CDK9, CRM1, HP68, and CIITA genes in the fused cells. We chose these genes for study because they have been suggested to affect HIV-1 replication (Herrmann and Rice, 1995; Chen et al., 1999; Saifuddin et al., 2000; Cmarko et al., 2002; Zimmerman et al., 2002; Lingappa et al., 2006). As shown in Fig. 4, expression of most human genes was lost or down-regulated after cell fusion. By contrast, expression of rat genes coding for cyclin T1, CDK9, CRM1, HP68, and CIITA was not altered (data not shown). These observations indicate that human genes are preferentially lost or inactivated by cell fusion. Some hybrid

Please cite this article as: Chen, J., et al., Enhanced production of p24 Gag protein in HIV-1-infected rat cells fused with uninfected human cells, Exp. Mol. Pathol. (2006), doi:10.1016/j.yexmp.2006.11.003

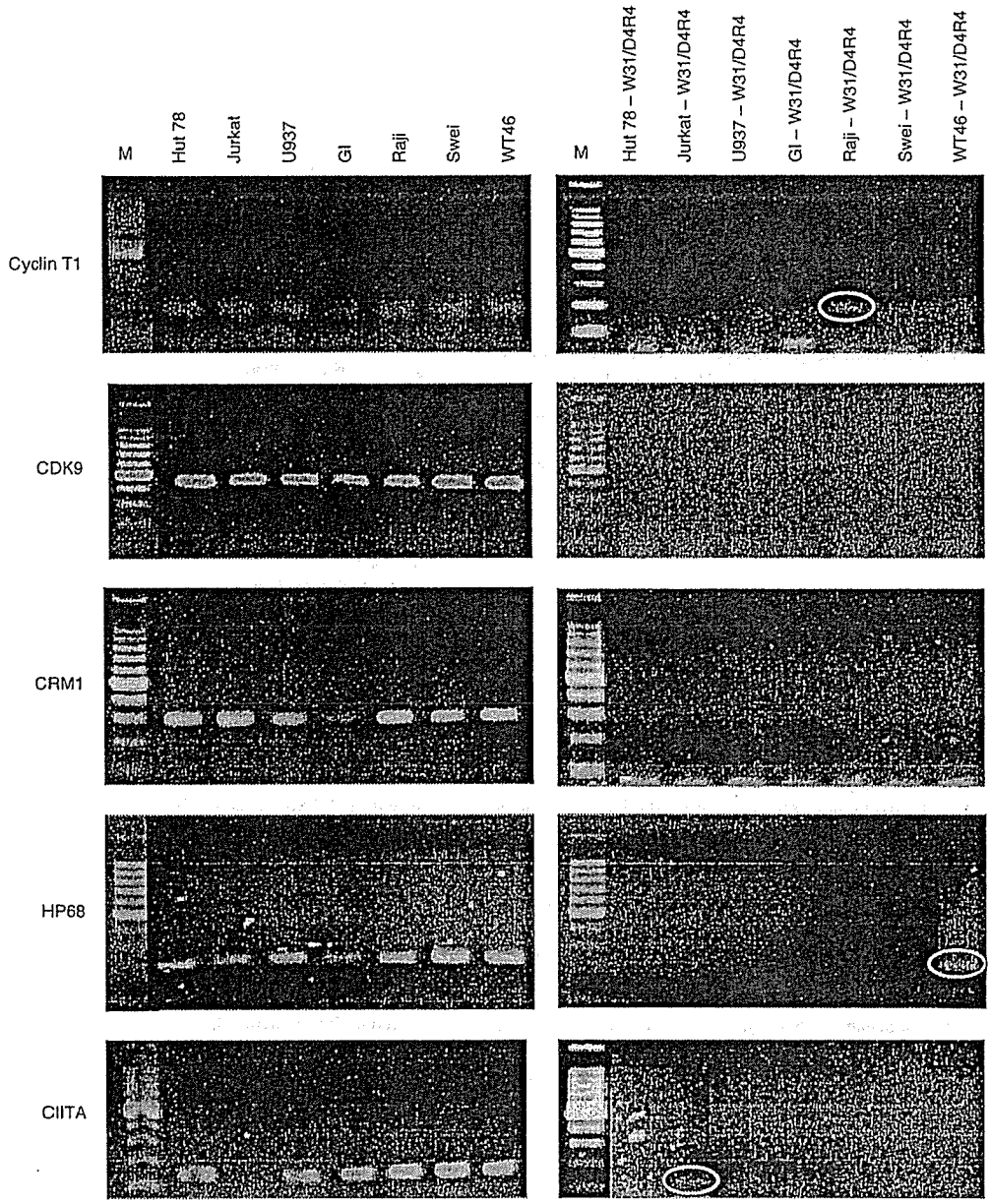


Fig. 4. Expression profiles of human genes in parental human cell lines (left) and hybrid cells (right). Expression of cyclin T1, CDK9, CRM1, HP68, and CIITA was examined by RT-PCR. Human cell lines were fused with HIV-1-infected W31/D4R4 cells. Total RNAs from hybrid cells were extracted at day 21 after fusion. The same hybrid cells were used for in Fig. 3 and this figure. The asterisk indicates that Jurkat cells did not express detectable amounts of CIITA. Ovals indicate specific PCR products. M, 100-bp ladder marker.

cells ceased to express all of the human genes examined, but still showed increased production of p24. This suggests that human molecules that facilitate HIV-1 replication are not limited to cyclin T1, CDK9, CRM1, HP68, and CIITA. There may be unknown human molecules that compensate for the loss of cyclin T1, CDK9, CRM1, HP68, and CIITA and promote HIV-1 replication.

Interestingly, fusion with Jurkat cells consistently failed to increase p24 production. This was not because the efficiency of cell fusion was low in Jurkat since we confirmed that all of the human cell lines examined in this study fused with W31/D4R4 cells with almost the same efficiency (data not shown). It was initially reported that CIITA might promote HIV-1 replication by functioning as a substitute of Tat during an initial post-infection period (Saifuddin et al., 2000). However, more recent work indicates that overexpression of CIITA inhibits viral replication by blocking the function of Tat (Okamoto et al., 2000; Accolla et al., 2002). In this regard, it is interesting to note that human CIITA, which was not expressed in Jurkat, began to be expressed after fusion with rat cells. Transcriptional induction of CIITA might be involved in poor production of p24 in W31/D4R4–Jurkat hybrid cells.

Please cite this article as: Chen, J., et al., Enhanced production of p24 Gag protein in HIV-1-infected rat cells fused with uninfected human cells, Exp. Mol. Pathol. (2006), doi:10.1016/j.yexmp.2006.11.003

A slight but significant increase in p24 concentration (10 pg/ml) was found in the supernatants of W31/D4R4–WT46 hybrid cells (Fig. 3B). Interestingly, expression of human HP68 was detected only in this hybrid cells. These results are consistent with the previous reports that human HP68 is a cellular protein important for capsid assembly (Zimmerman et al., 2002; Lingappa et al., 2006). Based on these findings, we suggest that introduction of human HP68 should be considered when designing animal models of HIV-1 infection.

In summary, we performed cell fusion experiments using HIV-1-infected rat fibroblasts and uninfected human cell lines of T-cell, B-cell, and macrophage lineages. Our results indicate that human cellular factors supporting HIV-1 replication are distributed in all of these cell lineages. Identification of additional factors affecting HIV-1 replication, the presence of which was suggested by the cell fusion experiments (Fig. 4), would be important to understand the replication cycle of HIV-1 and to develop countermeasures to control HIV-1 infection.

## Acknowledgment

This work was supported by a grant from The Japan Society for the Promotion of Science.

## References

Accolla, R.S., Mazza, S., Barbaro, A., De Maria, A., Tosi, G., 2002. The HLA class II transcriptional activator blocks the function of HIV-1 Tat and inhibits viral replication. Eur. J. Immunol. 32, 2783–2791.

Brandt, C.D., Rakusan, T.A., Sison, A.V., Josephs, S.H., Saxena, E.S., Herzog, K.D., Parrott, R.H., Sever, J.L., 1992. Detection of human immunodeficiency virus type 1 infection in young pediatric patients by using polymerase chain reaction and biotinylated probes. J. Clin. Microbiol. 30, 36–40.

Chen, D., Fong, Y., Zhou, Q., 1999. Specific interaction of Tat with the human but not rodent P-TEFb complex mediates the species-specific Tat activation of HIV-1 transcription. Proc. Natl. Acad. Sci. U. S. A. 96, 2728–2733.

Cmarko, D., Boe, S.O., Scassellati, C., Szilvay, A.M., Davanger, S., Fu, X.D., Haukenes, G., Kalland, K.H., Fakan, S., 2002. Rev inhibition strongly affects intracellular distribution of human immunodeficiency virus type 1 RNAs. J. Virol. 76, 10473–10484.

Freed, E.O., 2004. HIV-1 and the host cell: an intimate association. Trends Microbiol. 12, 170–177.

Herrmann, C.H., Rice, A.P., 1995. Lentivirus Tat proteins specifically associate with a cellular protein kinase, TAK, that hyperphosphorylates the carboxyl-terminal domain of the large subunit of RNA polymerase II: candidate for a Tat cofactor. J. Virol. 69, 1612–1620.

Kanki, K., Torigoe, T., Hirai, I., Sahara, H., Kamiguchi, K., Tamura, Y., Yagihashi, A., Sato, N., 2000. Molecular cloning of rat NK target structure—the possibility of CD44 involvement in NK cell-mediated lysis. Microbiol. Immunol. 44, 1051–1061.

Keppler, O.T., Yonemoto, W., Welte, F.J., Patton, K.S., Iacovides, D., Atchison, R.E., Ngo, T., Hirschberg, D.L., Speck, R.F., Goldsmith, M.A., 2001. Susceptibility of rat-derived cells to replication by human immunodeficiency virus type 1. J. Virol. 75, 8063–8073.

Kozak, S.L., Platt, E.J., Madani, N., Ferro, F.E.Jr., Peden, K., Kabat, D., 1997. CD4, CXCR-4, and CCR-5 dependencies for infections by primary patient and laboratory-adapted isolates of human immunodeficiency virus type 1. J. Virol. 71, 873–882.

Lingappa, J.R., Dooher, J.E., Newman, M.A., Kiser, P.K., Klein, K.C., 2006. Basic residues in the nucleocapsid domain of Gag are required for interaction of HIV-1 Gag with ABCE1 (HP68), a cellular protein important for HIV-1 capsid assembly. J. Biol. Chem. 281, 3773–3784.

Okamoto, H., Asamitsu, K., Nishimura, H., Kamatani, N., Okamoto, T., 2000. Reciprocal modulation of transcriptional activities between HIV-1 Tat and MHC class II transactivator CIITA. Biochem. Biophys. Res. Commun. 279, 494–499.

Pleskoff, O., Sol, N., Labrosse, B., Alizon, M., 1997. Human immunodeficiency virus strains differ in their ability to infect CD4+ cells expressing the rat homolog of CXCR-4 (fusin). J. Virol. 71, 3259–3262.

Saifuddin, M., Roebuck, K.A., Chang, Ch., Ting, J.P., Spear, G.T., 2000. Cutting edge: activation of HIV-1 transcription by the MHC class II transactivator. J. Immunol. 164, 3941–3945.

Sawada, S., Gowrishankar, K., Kitamura, R., Suzuki, M., Suzuki, G., Tahara, S., Koito, A., 1998. Disturbed CD4+ T cell homeostasis and in vitro HIV-1 susceptibility in transgenic mice expressing T cell line-tropic HIV-1 receptors. J. Exp. Med. 187, 1439–1449.

Tateno, M., Levy, J.A., 1988. MT-4 plaque formation can distinguish cytopathic subtypes of the human immunodeficiency virus (HIV). Virology 167, 299–301.

Trkola, A., 2004. HIV-host interactions: vital to the virus and key to its inhibition. Curr. Opin. Microbiol. 7, 407–411.

Yamamura, Y., Kotani, M., Chowdhury, M.I., Yamamoto, M., Yamaguchi, K., Karasuyama, H., Katsura, Y., Miyasaka, M., 1991. Infection of human CD4+ rabbit cells with HIV-1: the possibility of the rabbit as a model for HIV-1 infection. Int. Immunol. 3, 1183–1187.

York-Higgins, D., Cheng-Mayer, C., Bauer, D., Levy, J.A., Dina, D., 1990. Human immunodeficiency virus type 1 cellular host range, replication, and cytopathicity are linked to the envelope region of the viral genome. J. Virol. 64, 4016–4020.

Zimmerman, C., Klein, K.C., Kiser, P.K., Singh, A.R., Firestein, B.L., Riba, S.C., Lingappa, J.R., 2002. Identification of a host protein essential for assembly of immature HIV-1 capsids. Nature 415, 88–92.

Please cite this article as: Chen, J., et al., Enhanced production of p24 Gag protein in HIV-1-infected rat cells fused with uninfected human cells, Exp. Mol. Pathol. (2006), doi:10.1016/j.yexmp.2006.11.003

ELSEVIER

Journal of the Neurological Sciences 249 (2006) 7–12

Journal of the Neurological Sciences

www.elsevier.com/locate/jns

# MRI studies of spinal visceral larva migrans syndrome

Fujio Umehara [a,*], Hideki Ookatsu [a], Daisuke Hayashi [a], Akifumi Uchida [a], Yukari Douchi [a], Hisashi Kawabata [a], Rina Goto [a], Akihiro Hashiguchi [a], Eiji Matsuura [a], Ryuichi Okubo [a], Itsuro Higuchi [a], Kimiyoshi Arimura [a], Yukifumi Nawa [b], Mitsuhiro Osame [a]

[a] *Department of Neurology and Geriatrics, Kagoshima University Graduate School of Medical and Dental Sciences, Kagoshima University, Sakuragaoka 8-35-1, Kagoshima, 890-8520, Japan*

[b] *Parasitic Diseases Unit, Department of Infectious Diseases, Faculty of Medicine, University of Miyazaki, Miyazaki, 889-1692, Japan*

Received 2 November 2005; received in revised form 19 May 2006; accepted 19 May 2006
Available online 3 July 2006

**Abstract**

We report serial MR findings in four patients with myelitis caused by visceral larva migrans syndrome due to *Toxocara canis* or *Ascaris suum* infection. MR imaging revealed spinal cord swelling with or without gadolinium enhancement in three patients. T2-weighted images showed high signal intensities preferentially located in both lateral and posterior columns. Antihelmintic and corticosteroid treatment yielded improvement in neurologic deficits and spinal lesions. However, one patient with *T. canis* infection relapsed associated with reappearance of MRI abnormalities.


*Keywords:* Visceral larva migrans syndrome; *Toxocara canis*; *Ascaris suum*; Myelitis; MRI

## 1. Introduction

Visceral larva migrans (VLM) syndrome is a zoonotic disease caused by the migration or presence in human tissue of helminth larva from low-order animals. VLM syndrome most commonly affects the liver, skin, lungs and eyes [1], but involvement of the central nervous system is rare. The most common cause of VLM syndrome is the dog ascarid, *Toxocara canis* (*T. canis*) [2]. Prevalence of *T. canis* infection in dogs and the resulting ground contamination is relatively high in many countries. Recently, an outbreak of visceral larva migrans due to *Ascaris suum* (*A. suum*) infection has been reported in Kyushu, Japan [3].

Several reports of myelitis caused by VLM syndrome due to either *A. suum*, or *T. canis* infection have been reported [4–11]. However, long-term prognosis of the disease has not been well understood. In this paper, we report four cases of parasitic myelitis (2 patients with *T. canis* infection, and 2 patients with *A. suum* infection).

* Corresponding author. Tel.: +81 99 275 5332; fax: +81 99 265 7164.
*E-mail address:* umehara@m2.kufm.kagoshima-u.ac.jp (F. Umehara).

0022-510X/$ - see front matter © 2006 Elsevier B.V. All rights reserved.
doi:10.1016/j.jns.2006.05.057

## 2. Subjects and methods

For screening of parasite infection, multiple dot ELISA for 12 parasite antigens, *A. suum*, *T. canis*, *Dirofilaria immitis*, *Anisakis simplex*, *Gnathostoma doloresi*, *Strongyloides ratti*, *paragonimus westermanii*, *Paragonimus miyazakii*, *Fasciola hepatica*, *Clonorchis sinensis*, *Spirometra erinacei* and *Cysticercus cellulosae*, was performed. For evaluation of the treatment, semiquantitative analysis by microplate ELISA using antigens of *T. canis* and *A. suum* was done.

## 3. Case report

### 3.1. Patient 1

A 37-year-old woman who lived in Kagoshima prefecture in southern Kyusyu, Japan, noticed muscle convulsion of the right leg in December 2000. In January 2001, she had muscle weakness and dysesthesia of the left leg. Similar symptoms developed on the right leg from April 2001 resulting in paraplegia by May 2001. She was admitted to our clinic May 2001. On neurological

examination, she had spastic paraplegia associated with sensory impairment in all modalities below the T4 level. She also had urinary retention and bowel dysfunction. Deep tendon reflexes were exaggerated in both upper and lower limbs, and Babinski signs were positive bilaterally. Sagittal T1-weighted image (T1WI) revealed swelling of the cervical spinal cord (Fig. 1a). Sagittal T2-weighted image (T2WI) of the cervical and thoracic cord showed high signal intensity at the same levels (Figs. 1b, c). Brain MRI revealed a high intensity lesion in the left parietal white matter (Fig. 1d). Biochemical and hematological tests were normal except for eosinophilia (WBC: 6600/mm$^3$, eosinophil 11%, baso 1%, mono 4%, lympho 29%, neutro 55%). Cerebrospinal fluid examination disclosed the following results; mononuclear cells 38/mm$^3$, protein 149 mg/dl, glucose 43 mg/dl. Oligoclonal band was negative, and myelin basic protein was not elevated. At this point, she was diagnosed with an inflammatory myelitis of unknown etiology, and was started on intravenous methylprednisolone treatment (1000 mg/day for 3 days) followed by oral prednisolone treatment. Follow-up MRI revealed a decrease in the spinal cord swelling and high intensity signals. On multiple dot ELISA for 12 parasite antigens, both serum and CSF strongly bound to *T. canis* only. Parasite eggs were not found on repeated stool examinations. A diagnosis of myelitis caused by *T. canis* infection was then made. Albendazole (600 mg/day) was given for 2 courses of 4 weeks each with a 2-week interval between courses. Thereafter, high intensity signals in the spinal cord on T2WI remarkably decreased associated with improvement of muscle weakness in the lower limbs (Figs. 2a, b). Although she continued rehabilitation, she noticed worsening of paraparesis 6 months later. Spinal MRI revealed swelling of the spinal cord from the upper cervical to the lower thoracic cord levels with high intensity signals on T2WI (Figs. 2c, d). Cerebrospinal fluid examination disclosed the following; cells 53/mm$^3$ (eosinophils 1%, lymphocytes 94%, monocytes 5%), protein 150 mg/dl, glucose 43 mg/dl, and IgG index 0.82. Antibody titer to *T. canis* was not elevated. Again, she was treated with intravenous methylprednisolone (1000 mg/day for 3 days) followed by oral prednisolone. Although she became able to sit on a chair, severe paraparesis remained. Three weeks after, CSF examination revealed a decrease in cell count (21/mm$^3$), and protein (39 mg/dl). Repeat spinal MRI revealed marked reduction of spinal cord swelling with high intensity areas.

### 3.2. Patient 2

A 40-year-old woman who lived in Kagoshima prefecture, in southern Kyusyu, Japan, noticed acute hypoesthesia and dysesthesia in the lower limbs on June 9, 2003. One week later, muscle weakness in the right lower limb developed and then worsened. She visited us in July of the same year. On neurological examination, she had spastic paraplegia (predominantly in the right lower limb) associated with superficial sensory impairment below the T10 level, although deep sensation was preserved. She had urinary retention and bowel dysfunction. Deep tendon reflexes were exaggerated in the

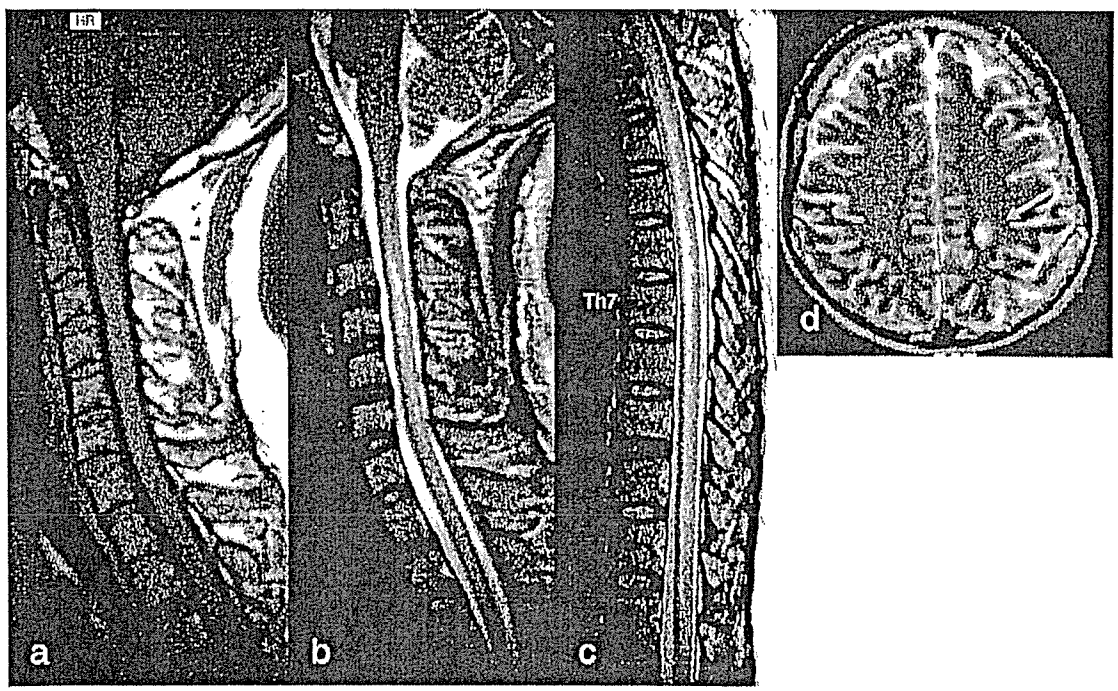


Fig. 1. MRI before treatment (patient 1). (a) Sagittal T1-weighted image (T1WI) demonstrating swelling of the cervical spinal cord. (b, c) Sagittal T2-weighted image (T2WI) showing high signal intensity in the entire spinal cord. (d) Brain MRI demonstrating a high signal intensity area in the left parietal white matter.

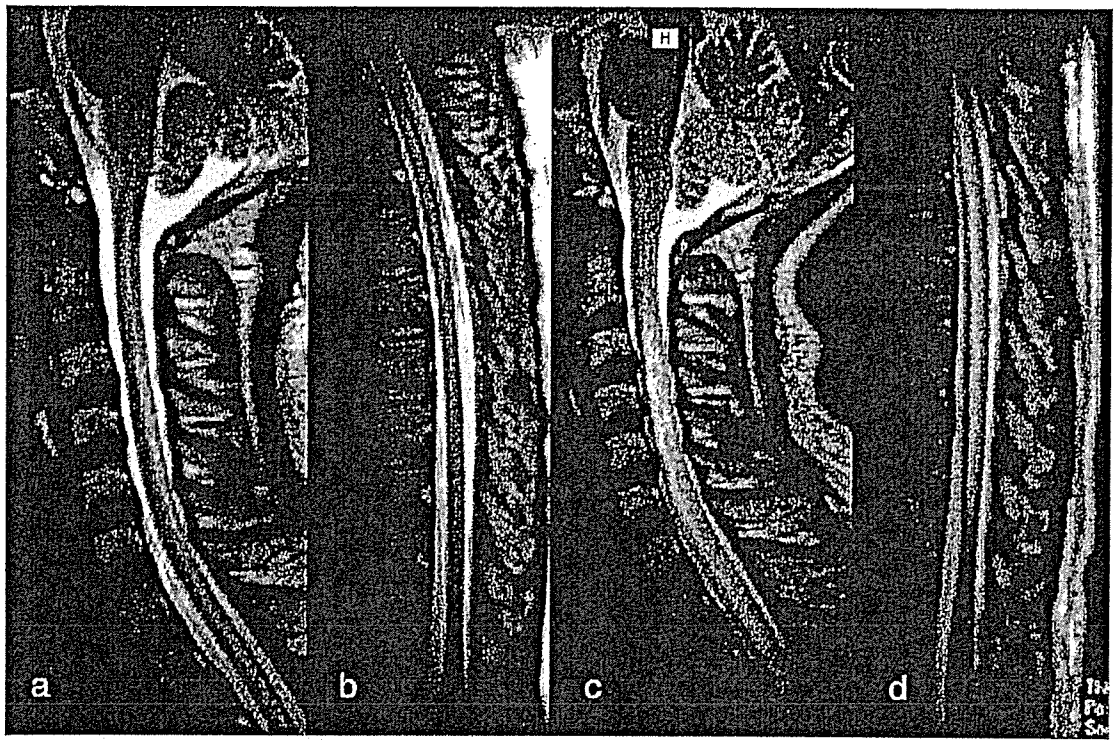


Fig. 2. Follow-up MRI after treatment (patient 1). (a) Sagittal T2WI shows improvement but still residual high-signal intensity in the posterior aspects of the cervical cord. (b) Sagittal T2WI showing disappearance of the high signal intensity area in the thoracic cord. (c, d) On relapse, sagittal T2WI showing swelling with high intensity signal throughout the spinal cord.

lower limbs and Babinski signs were positive bilaterally. Lhermitte's sign was positive. Her gait was unstable. Sagittal T1WI revealed swelling of the spinal cord from T1 to T7 (Fig. 3a). Sagittal T2WI revealed high signal intensity at the corresponding levels (Fig. 3b). After the administration of gadolinium, focal enhancement was noted (Figs. 3c, d). Brain

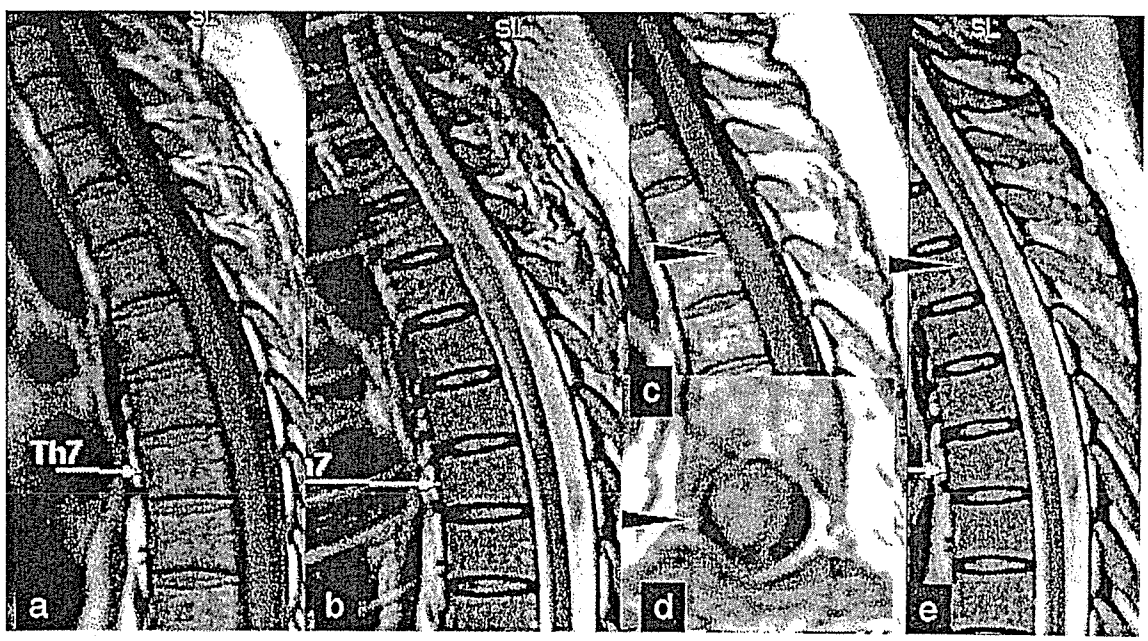


Fig. 3. MRI before (a–d) and after (e) treatment (patient 2). (a) Sagittal T1WI demonstrates swelling of the cord from T3 to T6. (b) Sagittal T2WI shows high signal intensity in the same levels. (c, d) Post-contrast sagittal (c) and axial (d) T1WI show focal enhancement at the T4 level (arrowhead). (e) After the second treatment, sagittal T2WI showing decreased swelling with residual high signal intensity of the spinal cord.

MRI was unremarkable. Biochemical and hematological tests were normal except for hyper IgEemia (802 IU/ml, normal 3–304 IU/ml). Cerebrospinal fluid examination disclosed the following: cells 9/mm$^3$ (eosinophils 10%, mononuclear cells 90%), protein 31 mg/dl, glucose 43 mg/dl, IgG index 0.73. Oligoclonal band was negative, and myelin basic protein was not elevated. At this point, she was diagnosed with an inflammatory myelitis of unknown etiology, and then had intravenous methylprednisolone treatment (1000 mg/day for 3 days) followed by oral prednisolone treatment. Follow-up MRI revealed decrease of spinal cord swelling and high intensity signals. On multiple dot ELISA, both serum and CSF strongly bound to *T. canis* and *A. suum*, and weakly to *Dirofilaria immitis*, *Anisakis simplex*, *Gnathostoma doloresi*, and *Strongyloides ratti*. Microplate ELISA was positive for positive for *T. canis* only. Parasite eggs were not found on repeated stool examinations. A diagnosis of myelitis caused by *T. canis* infection was then made. Albendazole (600 mg/day) with oral prednisolone (30 mg/day) was given daily for 2 courses of 4 weeks each with a 2-week interval between each course. Thereafter, high intensity signals in the spinal cord on T2WI remarkably decreased (Fig. 3e) associated with improvement of muscle weakness in the lower limbs.

### 3.3. Patient 3

A 54-year-old man who lived in Kagoshima prefecture, noticed muscle weakness in the right lower limb, and numbness in bilateral lower limbs on April 15, 2003. Three days later, he had facial numbness followed 5 days later by muscle weakness in the lower limbs. He consulted us April 28, 2003. On neurological examination, he had spastic paraplegia associated with numbness of the face and extremities. He also had urinary retention and bowel dysfunction. Deep tendon reflexes were exaggerated in both upper and lower limbs; however, Babinski signs were negative bilaterally. Sagittal T2WI showed high signal intensity at the spinal cord from C2 to T3 (Fig. 4a) without gadolinium enhancement. Brain MRI was unremarkable. Biochemical and hematological tests were normal except for eosinophilia (WBC: 4700/mm$^3$, eosinophil 8%, baso 2%, mono 6%, lympho 38%, neutro 46%) and hyper IgEemia (991 IU/ml). Cerebrospinal fluid examination disclosed a normal cell count 2/mm$^3$ (mononuclear cell), protein 38 mg/dl, glucose 43 mg/dl. Oligoclonal band was negative, and myelin basic protein was not elevated. EEG showed disorganization of α wave activity, and spikes after hyperventilation. On multiple dot ELISA, both serum and CSF strongly bound to *A. suum* only. Parasite eggs were not found on repeated stool examinations. At this point, she was diagnosed myelitis caused by *A. suum* infection. She was given daily for 2 courses of 4 weeks each with a 2-week interval between courses. Thereafter, there was improvement of muscle weakness in the lower limbs associated with decrease of high intensity signals in the cervical cord on MRI (Fig. 4b).

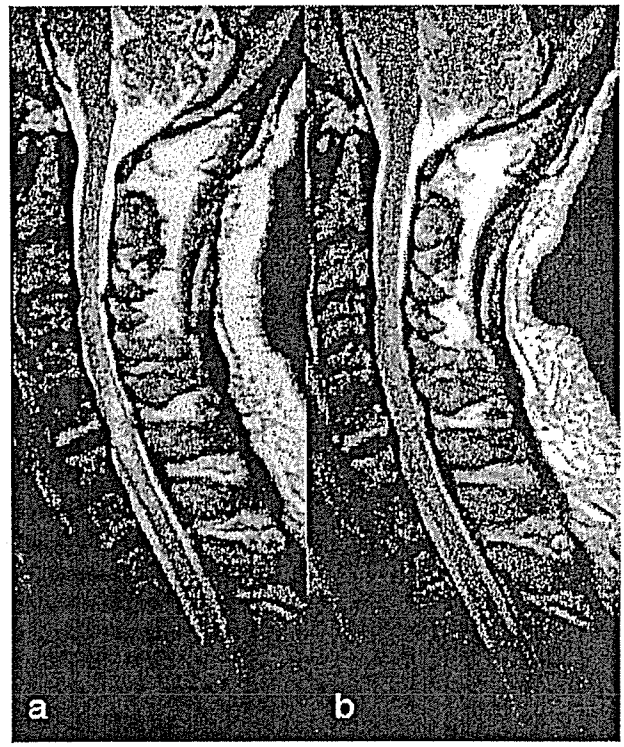


Fig. 4. MRI before (a) and after (b) treatment (patient 3). (a) Sagittal T2WI demonstrates high signal intensity and swelling of the spinal cord from C2 to T3. (b) Sagittal T2WI shows remarkable decrease in high signal intensity.

### 3.4. Patient 4

A 29-year-old man who lived in Kagoshima prefecture, suddenly noticed numbness in bilateral lower limbs on April 15, 2003. Three days later, he had numbness of the face followed 5 days later by muscle weakness in the lower limbs. He consulted us on April 28, 2003. On neurological examination, he had spastic paraplegia associated with numbness of the face and extremities. He also had urinary retention and bowel dysfunction. Deep tendon reflexes were exaggerated in both upper and lower limbs; however, Babinski signs were negative bilaterally. Spinal and Brain MRI were unremarkable. Biochemical and hematological tests were normal except for eosinophilia (WBC: 4700/mm$^3$, eosinophil 8%, baso 2%, mono 6%, lympho 38%, neutro 46%) and hyper IgEemia (991 IU/ml). Cerebrospinal fluid examination disclosed the following results: normal cell count 2/mm$^3$ (mononuclear cell), protein 38 mg/dl, glucose 43 mg/dl. Oligoclonal band was negative, and myelin basic protein was not elevated. EEG showed disorganization of α wave activity, and spikes after hyperventilation. On multiple dot ELISA, both serum and CSF strongly bound to *A. suum* only. Parasite eggs were not found in repeated stool examinations. At this point, she was diagnosed with myelitis caused by *A. suum* infection. She had intravenous methylprednisolone treatment (1000 mg/day for 3 days) followed by oral prednisolone treatment.

Albendazole (600 mg/day) was given for 2 courses of 4 weeks each with a 2-week interval between courses. Thereafter, there was improvement of muscle weakness in the lower limbs.

## 4. Discussion

The four patients presented were diagnosed with parasitic myelitis. In patients 1, 2, the cause was *T. canis* infection. *T. canis* is an unusual cause of myelopathy, most probably resulting from hematogenous infestation of the spinal cord with *T. canis* larvae. MRI findings in patient 1 revealed swelling of the spinal cord with high intensity lesions involving whole spinal cord. In patient 2, similar abnormalities were found at T1–T7 levels with focal gadolinium enhancement. These changes resolved soon after the starting antihelmintic and corticosteroid therapy. The pathogenesis of myelitis due to larva migrans syndrome is not well understood. Ascarid larvae have been reported to survive longer in the parenchymatous tissue and secrete antigens that cause allergic reactions in hosts. Albendazole was therefore considered to have directly killed the larvae, and albendazole with corticosteroid jointly suppressed the host's allergic reactions.

Patient 1 developed relapsing symptoms associated with re-appearance of spinal MRI abnormalities. Fluctuation of symptoms associated with MRI abnormalities in patients with *T. canis*-myelopathy has never been reported in the literature. During the second attack, antibody for *T. canis* did not increase in CSF, but cell count, protein and MBP were elevated. These findings suggest that allergic reactions in the CNS may have played a major role in the inflammation of the spinal cord in patient 1.

There are only a few reports on MRI findings of myelitis due to *T. canis* (7, 8, 9, 10). Swelling and high signal intensities in the spinal cord, as shown in the present cases, are common. Nevertheless, there were some unusual features in these cases. In patient 1, although the entire spinal cord was swollen, high intensity signals were located both posteriorly and laterally in the cord. Preferential location of residual damage within the posterior columns has been reported in *T. canis*-myelopathy [7]. Clearly symmetrical residual damage confined to both lateral and posterior columns in patient 1 strongly suggests a specific vulnerability of these structures to in this myelopathy. In contrast, high intensity signals were preferentially located in the right lateral columns of the thoracic cord, which are compatible with the neurological symptoms in patient 2. Taken together, both symmetrical and asymmetrical high intensity signals with or without Gd enhancement on spinal MRI could be observed in *T. canis*-myelopathy.

In patients 3, 4, the myelopathy may have been caused by *A. suum* infection. Myelopathy due to *A. suum* infection is rare [6]. In areas where it is endemic, infection with *A. suum* occurs primarily from ingesting vegetables contaminated with pig manure containing parasite eggs. Both patients lived in Kagoshima, an endemic area for *A. suum* infection. In addition, some patients were assumed to be infected by eating raw beef or chicken (liver or meat), contaminated with *A. suum* larvae. Patient 3 had a habit of eating raw beef or chicken meat.

There are two reports describing MRI findings of CNS lesions in patients with *A. suum* infection. In a patient with encephalopathy, there were many Gd-DTPA enhanced lesions in the cerebral cortex on T1WI and diffuse, symmetrical lesions in the cerebral white matter on fluid attenuated inversion recovery (FLAIR) images [12,13]. In a patient with myelopathy, a high signal intensity lesion at the $Th_1$ spine level on T2WI, which enhanced after gadolinium administration was reported [6]. In the present study, patient 3 showed similar findings from the cervical to the upper thoracic cord levels; however, there were no significant abnormalities in the spinal cord of patient 4. These findings suggest that negative MRI findings do not exclude a possibility of myelopathy caused by *A. suum* or other parasitic infections.

In conclusion, spinal "visceral larva migrans" syndrome caused by *T. canis* or *A. suum* should be considered as one of the differential diagnosis of myelopathy with unknown etiology. Multiple dot ELISA is useful for screening, and semiquantitative analysis by microplate ELISA using antigens *is informative for* evaluation of the treatment.

## Acknowledgement

We thank Dr. Arlene R. Ng for critical reading of the manuscript.

## References

[1] Glickman LT, Schantz PM. Epidemiology and pathogenesis of zoonotic Toxocariasis. Epidemiol Rev 1981;3:230–50.
[2] Ruttinger P, Hadidi H. MRI in cerebral toxocaral disease. J Neurol Neurosurg Psychiatry 1991;54:361–2.
[3] Maruyama H, Nawa Y, Noda S, Mimori Choi WY. An outbreak of visceral larva migrans due to *Ascaris suum* in Kyusyu, Japan. Lancet 1996;347:1766–7.
[4] Yoshida S, Matsui M, Wang HY, Oeda T, Sasaki T, Komure O, et al. A case of myeloradiculitis as a complication of visceral larva migrans due to *Ascaris suum*. Rinsho Shinkeigaku 2004;44:198–202.
[5] Kawajiri M, Osoegawa M, Ohyagi Y, Ochi H, Furuya H, Nawa Y, et al. A case of myeloradiculitis as a complication of visceral larva migrans due to *Ascaris suum*. Rinsho Shinkeigaku 2004;44: 198–202.
[6] Osoegawa M, Matsumoto S, Ochi H, Yamasaki K, Horiuchi I, Kira YO, et al. Localised myelitis caused by visceral larva migrans due to *Ascaris suum* masquerading as an isolated spinal cord tumor. J Neurol Neurosurg Psychiatry 2001;70:265–6.
[7] Duprez TP, Bigaignon G, Delgrange E, Desfontaines P, Hermans M, Vervoort T, et al. MRI of cervical cord lesions and their resolution in *Toxocara canis* myelopathy. Neuroradiology 1996;38:792–5.
[8] Goffette S, Jeanjean AP, Duprez TP, Bigaignon G, Sindic CJ. Eosinophilic pleocytosis and myelitis related to *Toxocara canis* infection. Eur J Neurol 2000;7:703–6.
[9] Kumar J, Kimm J. MR in *Toxocara canis* myelopathy. Am J Neuroradiol 1994;15:1918–20.
[10] Duprez TP, Bigaignon G, Delgrange E, Desfontaines P, Hermans M, Vervoort T, et al. MRI of cervical cord lesions and their resolution in *Toxocara canis* myelopathy. Neuroradiology 1996;38:792–5.

[11] Vidal JE, Sztajnbok J, Seguro AC. Eosinophilic meningoencephalitis due to *Toxocara canis*: case report and review of the literature. Am J Trop Med Hyg 2003;69:341–3.
[12] Inatomi Y, Murakami T, Tokunaga M, Ishiwata K, Nawa Y, Uchino M. Encephalopathy caused by visceral larva migrans due to *Ascaris suum*. J Neurol Sci 1999;164:195–9.
[13] Xinou E, Lefkopoulos A, Gelagoti M, Drevelegas A, Diakou A, Milonas I, et al. CT and MR imaging findings in cerebral toxocaral disease. Am J Neuroradiol 2003;24:714–8.

ELSEVIER

Journal of the Neurological Sciences 241 (2006) 103 – 106

Journal of the Neurological Sciences

www.elsevier.com/locate/jns

Short communication

# Chronic progressive sensory ataxic neuropathy associated with limited systemic sclerosis

Yasuyuki Nobuhara *, Mineki Saito, Rina Goto, Yoshihito Yoshidome, Miwako Kawamura, Takefumi Kasai, Ikkou Higashimoto, Nobutaka Eiraku, Fujio Umehara, Mitsuhiro Osame, Kimiyoshi Arimura

*Department of Neurology and Respiratory Disease, Kagoshima University Hospital, 8-35-1 Sakuragaoka, Kagoshima 890-8520, Japan*

Received 24 August 2005; accepted 18 October 2005
Available online 5 December 2005

**Abstract**

We report the case of a 33-year-old woman with limited systemic sclerosis and chronic progressive sensory ataxic neuropathy. Sural nerve biopsy showed loss of myelinated fibers mostly those of large diameter, axonal degeneration and infiltration of macrophages, but no signs of vasculitis. Physical examination, laboratory testing, neurophysiological and neuroradiological examinations suggested that the dorsal root was primarily affected in this patient. Cytokine analysis by multiplex bead array assay revealed that IL-1β and GM-CSF were increased both in serum and CSF. Although her symptoms did not respond to corticosteroid therapy, intravenous immunoglobulin (IVIg) therapy resulted in marked improvement. IVIg could be effective in case of immune-mediated reversible neuronal dysfunction associated with collagen disease without vasculitis.


*Keywords:* Chronic progressive sensory ataxic neuropathy; Limited systemic sclerosis; Intravenous immunoglobulin (IVIg); IL-1β; GM-CSF

## 1. Introduction

Neuropathies are a common neurologic manifestation of diffuse connective tissue disease, and are mainly due to ischemia caused by systemic vasculitis [1]. Systemic sclerosis (SSc) is also a connective tissue disease characterized by abundant fibrosis of the skin, blood vessels, and visceral organs [2]. Although clinical peripheral nervous system disease is regarded as uncommon in SSc [3], recent studies demonstrated that neurological involvement in SSc is more frequent than has been assumed [4]. The most commonly observed neurologic manifestations in SSc are mononeuritis multiplex, trigeminal neuropathy and entrapment neuropathies, such as carpal tunnel syndrome [3]. However, since limited SSc is relatively stable and localized, as opposed to generalized SSc, neurological complications associated with it are rarely reported. Here we report the case of a 33-year-old-woman with limited SSc, complicated by chronic progressive sensory ataxic neuropathy (CSAN) characterized by insidious onset and slowly progressive sensory impairment. Although her symptoms did not respond to corticosteroid therapy, marked improvement was achieved by intravenous immunoglobulin (IVIg) therapy. The pathogenic background and underlying mechanism for efficacious IVIg therapy in this case are discussed.

## 2. Patient and methods

### 2.1. Case history

A 33-year-old Japanese woman was admitted to our department for 9 months after the onset of finger swelling with early morning stiffness and Raynaud's phenomenon.

* Corresponding author. Present address: Department of Neurology, National Hospital Organization Okinawa Hospital, 3-20-4 Ganeko, Ginowan 901-2214, Japan. Tel.: +81 98 898 2121; fax: +81 98 897 9838.
*E-mail address:* nbh@m.kufm.kagoshima-u.ac.jp (Y. Nobuhara).

0022-510X/$ - see front matter © 2005 Elsevier B.V. All rights reserved.
doi:10.1016/j.jns.2005.10.010